

η' and η mesons with connection to anomalous glue

Steven D. Bass*

*Kitzbühel Centre for Physics, Kitzbühel, Austria
and Marian Smoluchowski Institute of Physics,
Jagiellonian University, PL 30-348 Krakow, Poland*

Pawel Moskal†

*Marian Smoluchowski Institute of Physics,
Jagiellonian University, PL 30-348 Krakow, Poland* (published 15 February 2019)

A review of the present understanding of η' and η meson physics and these mesons as a probe of gluon dynamics in low-energy QCD is presented. Recent highlights include the production mechanism of η and η' mesons in proton-nucleon collisions from threshold to high energy, the η' effective mass shift in the nuclear medium, searches for possible η and η' bound states in nuclei, as well as precision measurements of η decays as a probe of light-quark masses. Recent experimental data, theoretical interpretation of the different measurements, and the open questions and challenges for future investigation are discussed.

DOI: [10.1103/RevModPhys.91.015003](https://doi.org/10.1103/RevModPhys.91.015003)

CONTENTS

I. Introduction	1
II. QCD Symmetries and the η and η'	3
III. The Strong CP Problem and Axions	8
IV. η and η' Decays	9
A. Hadronic decays	9
B. Two-photon interactions	9
C. Precision tests of fundamental symmetries	11
V. η - and η' -nucleon Interactions	11
A. The $N^*(1535)$ resonance and its structure	14
VI. The η and η' in Nuclei	14
A. The η' in medium	15
B. η mesic nuclei	16
C. The η' at finite temperature	17
VII. High-energy η and η' Production	17
A. η' - π interactions and 1^{-+} exotics	18
VIII. Summary and Future Challenges	19
Acknowledgments	19
References	19

I. INTRODUCTION

The η' meson is special in quantum chromodynamics (QCD), the theory of quarks and gluons, because of its strong affinity to gluons. Hadrons, their properties and interactions, are emergent from more fundamental QCD quark and gluon degrees of freedom. QCD has the property of asymptotic freedom. The coupling $\alpha_s(P^2)$ which describes the strength of quark-gluon and gluon-gluon interactions decreases logarithmically with increasing (large) four-momentum transfer squared, P^2 . In the infrared, at low P^2 , quark-gluon interactions become strong. Quarks become confined inside

hadron bound states and the vacuum is not empty but characterized by the formation of quark and gluon condensates. The physical degrees of freedom are emergent hadrons (protons, mesons, etc.) as bound states of quarks and gluons. Baryons such as the proton are bound states of three valence quarks. Mesons are bound states of a quark and an antiquark.

Glue is manifest in the confinement potential which binds the quarks. This confinement potential corresponds to a restoring force of 10 ton regardless of separation. Quarks are bound by a string of glue which can break into two colorless hadron objects involving the creation of a quark-antiquark pair corresponding to the newly created ends of two confining strings formed from the original single string of confining glue. There are no isolated quarks. The QCD confinement radius is of the order of 1 fm = 10^{-15} m. This physics at large coupling is beyond QCD perturbation theory and described either using QCD inspired models of hadrons which build in key symmetries of the underlying theory or through computational lattice methods. About 99% of the mass of the hydrogen atom, 938.8 MeV, is associated with the confinement potential with the masses of the electron 0.5 MeV and the proton 938.3 MeV. Inside the proton the masses of the proton's constituent two up quarks and one down quark are about 2.2 MeV for each up quark and 4.7 MeV for the down quark.

Besides generating the QCD confinement potential, glue plays a special role in the light-hadron spectrum through the physics of the isoscalar η' and η mesons including their interactions. The QCD Lagrangian with massless quarks is symmetric between left- and right-handed quarks (which are fermions) or between positive and negative helicity quarks. However, this symmetry is missing in the ground state hadron spectrum. The lightest mass hadrons, pions and kaons, are pseudoscalar mesons called Goldstone bosons associated with the spontaneous breaking of chiral symmetry between left- and right-handed quarks. These mesons are special in that the

*Steven.Bass@cern.ch

†P.Moskal@uj.edu.pl

squares of their masses are proportional to the masses of their constituent valence quark-antiquark pair. (In contrast, the leading term in the masses of the proton and spin-one vector mesons is determined by the confining gluonic potential with contributions from the light-quark masses treated as small perturbations.) The lightest mass pions, the neutral π^0 with mass 135 MeV and charged π^\pm with mass 140 MeV, play an important role in nuclear physics and the nucleon-nucleon interaction. The isosinglet partners of the pions and kaons, the pseudoscalar η and η' mesons, are too massive by about 300–400 MeV for them to be pure Goldstone states. They receive extra mass from nonperturbative gluon dynamics through a quantum effect called the axial anomaly. This glue comes with nontrivial topology. The physics of Goldstone bosons and the axial anomaly are explained in Sec. II. Gluon topology is an effect beyond the simplest quark models and involves non-local and long range properties of the gluon fields. Theoretical understanding of the η and η' involves subtle interplay of local symmetries and nonlocal properties of QCD. Examples of topology in other branches of physics include the Bohm-Aharonov effect and topological phase transitions and phases of matter in condensed matter physics, the 2016 Nobel Prize for Physics.

The η and η' mesons come with rich phenomenology. The η' is predominantly a flavor-singlet state. This means that its wave function is approximately symmetric in the three lightest quark types (up, down, and strange) that build up light-hadron spectroscopy. These different species of quarks couple to gluons with equal strength. The η' meson has strong coupling to gluonic intermediate states in hadronic reactions from low through to high energies. An example from high-energy reactions is the decay $J/\Psi \rightarrow \eta'\gamma$. The J/Ψ is made of a heavy charm-anticharm quark pair with mass 3686 MeV. Its decay to the light-quark η' meson plus a photon involves the annihilation of the charm-anticharm quark pair into a gluonic intermediate state which then forms the η' meson made of a near symmetric superposition of light quark-antiquark pairs (up-antiup, down-antidown, and strange-antistrange).

In this review we will discuss the broad spectrum of processes involving the η' that are mediated by gluonic intermediate states. The last 20 years has seen a dedicated program of η' and η meson production experiments from nucleons and nuclei close to threshold as well as in high-energy collisions. Studies of η and η' meson production and decay processes combine to teach us about the interface of glue and chiral dynamics, the physics of Goldstone bosons, in QCD. Measurements of η and η' production in nuclear media are sensitive to the behavior of fundamental QCD symmetries at finite density and temperature. In finite density nuclear media, for example, in nuclei and neutron stars, hadrons propagate in the presence of long range mean fields that are created by nuclear many body dynamics. Interaction with the mean fields in the nucleus can change the hadrons' observed properties, e.g., their effective masses, magnetic moments, and axial charges. Symmetries between left- and right-handed quarks, which are spontaneously broken in the ground state, are partially restored in nuclear media with a reduced size of the quark condensate. At large finite temperature there is an effective renormalization of the QCD coupling which

becomes reduced relative to the zero temperature theory for the same four-momentum transfer squared. One expects changes in hadron properties in the interaction region of finite temperature heavy-ion collisions. This review surveys η and η' meson physics as a probe of QCD dynamics emphasizing recent advances from experiments and theory.

In addition to the topics discussed here, the physics of glue in QCD features in many frontline areas of QCD hadron physics research. The planned electron ion collider has an exciting program to study the role of glue in nucleons and nuclei over a broad range of high-energy kinematics (Accardi *et al.*, 2016; Deshpande, 2017). The search for hadrons containing explicit gluon degrees of freedom in their bound state wave functions is a hot topic in QCD spectroscopy, e.g., possible glueball states built of two or three valence gluons and hybrids built of a quark-antiquark pair and a gluon (Klempt and Zaitsev, 2007). Gluons in the proton play an essential role in understanding the proton's internal spin structure (Aidala *et al.*, 2013). Studies of the QCD phase diagram (Braun-Munzinger and Wambach, 2009) from high density neutron stars (Lattimer and Prakash, 2016) to high temperature quark-gluon plasma and a color-glass condensate postulated to explain high density gluon matter in high-energy collisions (Gyulassy and McLerran, 2005) are hot topics at the interface of nuclear and particle physics research. On the theoretical side, much effort is invested in trying to understand the detailed dynamics which leads to the QCD confinement potential (Greensite, 2011).

The plan of this paper is as follows. In Sec. II we introduce the key theoretical issues with the η and η' mesons and their unique place at the interface of chiral and nonperturbative gluon dynamics. Here we explain the different gluonic effects at work in η and η' meson physics and how they are incorporated in theoretical calculations.

Section III discusses the strong CP puzzle. The observed matter-antimatter asymmetry in the Universe requires some extra source of CP violation beyond the quark mixing described by the Cabibbo-Kobayashi-Maskawa (CKM) matrix in the electroweak standard model. The nonperturbative glue which generates the large η' mass also has the potential to break CP symmetry in the strong interactions. This effect would be manifest as a finite neutron electric dipole moment proportional to a new QCD parameter θ_{QCD} , which is experimentally constrained to be very small, less than 10^{-10} . One possible explanation for the absence of CP violation here involves a new light-mass pseudoscalar particle called the axion. The axion is also a possible dark matter candidate to explain the “missing mass” in the Universe. While no axion particle has so far been observed, these ideas have inspired a vigorous program of ongoing experimental investigation to look for them.

Sections IV–VII focus on η and η' phenomenology. In Sec. IV we discuss the information about QCD which follows from η and η' decay processes. The amplitude for the η meson to three pions decay depends on the difference between the lightest up and down quark masses and provides valuable information about the ratio of light-quark masses. Studies of η and η' decays tell us about their internal quark-gluon and spatial structure. In addition, searches for rare decay processes provide valuable tests of fundamental symmetries.

Section V discusses η and η' production in near-threshold proton-nucleon collisions. The experimental program on η and η' nucleon interactions has focused on near-threshold meson production in proton-nucleon collisions and photoproduction from proton and deuteron targets (Moskal *et al.*, 2002; Krusche and Wilkin, 2015; Metag, Nanova, and Paryev, 2017; Wilkin, 2017). Recent highlights include the use of polarization observables in photoproduction experiments to search for new excited nucleon resonances (Anisovich *et al.*, 2017), measurement of the η' nucleon scattering length through the final state interaction in proton-proton collisions (Czerwinski *et al.*, 2014), and measurement of the spin analyzing power to probe the partial waves associated with η production dynamics in proton-proton collisions (Adlarson *et al.*, 2018b).

Section VI deals with the η and η' in QCD nuclear media and the formation of possible meson-nucleus bound states. Recent photoproduction experiments in Bonn have revealed an η' effective mass shift in nuclear medium, which is about -40 MeV at nuclear matter density (Novano *et al.*, 2013). Studies of the transparency of the nuclear medium to the propagating η' allow one to make a first (indirect) measurement of the η' -nucleus optical potential. One finds a small width of the η' in medium (Novano *et al.*, 2012) compared to the depth of the optical potential meaning that the η' may be a good candidate for possible bound state searches in finite nuclei.

Mesic nuclei, if discovered in experiments, are a new exotic state of matter involving the meson being bound inside the nucleus purely by the strong interaction, without electromagnetic Coulomb effects playing a role. Strong attractive interactions between the η meson and nucleons mean that both the η and η' are prime targets for mesic nuclei searches, with a vigorous ongoing program of experiments in both Europe and Japan (Metag, Novano, and Paryev, 2017). Searches for possible η mesic nuclei are focused on helium while searches for η' bound states are focused on carbon and copper.

The η' effective mass shift in nuclei of about -40 MeV at nuclear matter density is in excellent agreement with the prediction of the quark meson coupling model (Bass and Thomas, 2006) which works through coupling of the light up and down quarks in the meson to the σ (correlated two pion) mean field inside the nucleus. Here the η' experiences an effective mass shift in nuclei which is catalyzed by its gluonic component (Bass and Thomas, 2014). Without this glue, the η' would be a strange quark state after SU(3) breaking with small interaction with the σ mean field inside the nucleus.

Shifting from finite density to finite temperature, there are also hints in data from the Relativistic Heavy-Ion Collider (RHIC) for possible η' mass suppression at finite temperature, with claims of at least -200 MeV mass shift (Csorgo, Vertesi, and Sziklai, 2010; Vertesi, Csorgo, and Sziklai, 2011).

Section VII discusses η and η' production in high-energy hadronic scattering processes from light-quark hadrons. The ratio of η to π meson production at high transverse momentum p_t in high-energy proton-nucleus and nucleus-nucleus collisions is observed to be independent of the target nucleus in relativistic heavy-ion collision data from RHIC at Brookhaven

National Laboratory and the ALICE experiment at the Large Hadron Collider at CERN, indicating a common propagation mechanism through the nuclear medium in these kinematics. Interesting effects are also observed in high-energy η' production. The COMPASS experiment at CERN found that odd L exotic partial waves L^{-+} are strongly enhanced in $\eta'\pi$ relative to $\eta\pi$ exclusive production in collisions of 191 GeV negatively charged pions from hydrogen (Adolph *et al.*, 2015), consistent with expectations (Bass and Marco, 2002) based on gluon-mediated couplings of the η' .

In Sec. VIII we give conclusions and an outlook to possible future experiments which could shed new light on the structure and interactions of η and η' .

Earlier reviews on η and η' meson physics, each with a different emphasis, are given in the volume edited by Bijmens, Faldt, and Nefkens (2002). The lecture notes of Shore (2008) provide a theoretical overview of gluonic effects in η' physics. Axion physics is reviewed by Kawasaki and Nakayama (2013). Leutwyler (2013) discusses light-quark physics with a focus on the η meson and Kupsc (2009) gives an overview of the analysis of η and η' meson decays. Meson production in proton-proton collisions close to threshold is discussed in detail by Moskal *et al.* (2002), Krusche and Wilkin (2015), and Wilkin (2017). The present status of meson-nucleus interaction studies is reviewed by Metag, Novano, and Paryev (2017).

II. QCD SYMMETRIES AND THE η AND η'

Symmetries are important in hadron physics. Protons and neutrons with spin 1/2 are related through isospin SU(2), which is expanded to SU(3) to include Σ and Λ hyperons. Likewise, one finds SU(2) multiplets of spin-zero and spin-one mesons, e.g., the charged and neutral spin-zero pions are isospin partners and reside inside SU(3) multiplets together with kaons. This spectroscopy suggests that these hadronic particles are built from simpler constituents. These are spin 1/2 quarks labeled by SU(3) flavor quantum numbers up, down, and strange (denoted u , d , and s). These quarks carry electric charges $e_u = +2/3$ and $e_d, e_s = -1/3$ where, e.g., a proton is built from two up quarks and a down quark, and a neutron is built of two down quarks and an up quark. The spin-zero and spin-one mesons are built of a quark-antiquark combination. The hadron wave functions are symmetric in flavor-spin and spatial degrees of freedom. The Pauli principle is ensured with the quarks and antiquarks being antisymmetric in a new label called color SU(3), red, green, and blue.

High-energy deep inelastic scattering experiments probe the deep structure of hadrons by scattering high-energy electron or muon beams off hadronic targets. Deeply virtual photon exchange acts like a microscope which allows us to look deep inside the proton. One measures the inclusive cross section. These experiments reveal a proton built of nearly free fermion constituents, called partons.

The deep inelastic results and spectroscopy come together when color is made dynamical in the theory of QCD. Quarks carry a color charge and interact through colored gluon exchange, just like electrons interact through photon exchange in quantum electrodynamics (QED). QCD differs from QED in that gluons also carry color charge whereas photons are electrically neutral. [The dynamics is governed by the gauge

group of color SU(3) instead of U(1) for the photon.] This means that the Feynman diagrams for QCD include three gluon and four gluon vertices (as well as the quark gluon vertices) and that gluons self-interact. For excellent textbook discussions of QCD and its application to hadrons see [Close \(1979\)](#) and [Thomas and Weise \(2001\)](#).

Gluon-gluon interactions induce asymptotic freedom: the QCD version of the fine structure constant for quark-gluon and gluon-gluon interactions α_s decreases logarithmically with increasing resolution Q^2 . Gluon bremsstrahlung results in gluon induced jets of hadronic particles which were first discovered in high-energy e^-e^+ collisions at DESY ([Ellis, 2014](#)). Quark and gluon partons play a vital role in high-energy hadronic collisions, e.g., at the Large Hadron Collider at CERN ([Altarelli, 2013](#)). Deep inelastic scattering experiments also tell us that about 50% of the proton's momentum perceived at high Q^2 is carried by gluons, consistent with the QCD prediction for the deepest structure of the proton. QCD theory also predicts that about 50% of the proton's angular momentum budget at high Q^2 is contributed by gluon spin and orbital angular momentum ([Bass, 2005](#); [Aidala et al., 2013](#)).

Glue in low-energy QCD is manifest through the confinement potential which binds quarks inside hadrons. Color-singlet glueball excitations (bound states of gluons) as well as hybrid bound states of a quark and antiquark plus gluon are predicted by theory but still await decisive experimental confirmation.

The decay amplitude for $\pi^0 \rightarrow 2\gamma$ and the ratio of cross sections for hadron to muon-pair production in high-energy electron-positron collisions $R_{e^+e^-}$ are proportional to the number of dynamical colors N_c , giving an experimental confirmation of $N_c = 3$.

This dynamics is encoded in the QCD Lagrangian. We first write the quark field ψ as the sum of left- and right-handed quark components $\psi = \psi_L + \psi_R$, where $\psi_L = (1/2)(1 - \gamma_5)\psi$ and $\psi_R = (1/2)(1 + \gamma_5)\psi$ project out different states of quark helicity. The vector gluon field is denoted A_μ^b . For massless quarks, the QCD Lagrangian reads

$$\mathcal{L}_{\text{QCD}} = \bar{\psi}_L i\gamma^\mu D_\mu \psi_L + \bar{\psi}_R i\gamma^\mu D_\mu \psi_R - \frac{1}{2} \text{Tr} G^{\mu\nu} G_{\mu\nu}. \quad (1)$$

Here $D_\mu \psi = (\partial_\mu - igA_\mu)\psi$ describes the quark-gluon interaction; $G^{\mu\nu} = \partial^\mu A^\nu - \partial^\nu A^\mu + gf_{abc}A_b^\mu A_c^\nu$ is the gluon field tensor with the last term here generating the three-gluon and four-gluon interactions. The quark-gluon dynamics is determined by requiring invariance under the gauge transformations

$$\begin{aligned} \psi &\rightarrow \mathcal{G}\psi, \\ A_\mu &\rightarrow \mathcal{G}A_\mu \mathcal{G}^{-1} + \frac{i}{g}(\partial_\mu \mathcal{G})\mathcal{G}^{-1}, \end{aligned} \quad (2)$$

where \mathcal{G} describes rotating the local color phase of the quark fields.

For massless quarks the left- and right-handed quarks transform independently under chiral rotations which rotate between up, down, and strange flavored quarks. Finite quark masses through the Lagrangian term $m\bar{\psi}\psi$ explicitly break the chiral symmetry by connecting left- and right-handed quarks,

$$\bar{\psi}\psi = \bar{\psi}_L\psi_R + \bar{\psi}_R\psi_L. \quad (3)$$

Quark chirality (-1 for a left-handed quark and $+1$ for a right-handed quark) and helicity are conserved in perturbative QCD with massless quarks.

Low-energy QCD is characterized by confinement and dynamical chiral symmetry breaking. There is an absence of parity doublets in the light-hadron spectrum. For example, the $J^P = \frac{1}{2}^+$ proton and the lowest mass $J^P = \frac{1}{2}^-$ N*(1535) nucleon resonance (that one would normally take as chiral partners) are separated in mass by 597 MeV. This tells us that the chiral symmetry for light u and d (and s) quarks is spontaneously broken.

Spontaneous symmetry breaking means that the symmetry of the Lagrangian is broken in the vacuum. One finds a nonvanishing chiral condensate connecting left- and right-handed quarks

$$\langle \text{vac} | \bar{\psi}\psi | \text{vac} \rangle < 0. \quad (4)$$

This spontaneous symmetry breaking induces an octet of light-mass pseudoscalar Goldstone bosons associated with SU(3) including the pions and kaons which are listed in [Table I](#) and also [before extra gluonic effects in the singlet channel discussed below [Eq. \(9\)](#)] a flavor-singlet Goldstone state.¹

The Goldstone bosons P couple to the axial-vector currents which play the role of Noether currents through

$$\langle \text{vac} | J_{\mu 5}^i | P(p) \rangle = -if_P^i p_\mu e^{-ip \cdot x} \quad (5)$$

with f_P^i the corresponding decay constants (which determine the strength for $\pi^- \rightarrow \mu^- \bar{\nu}_\mu$) and satisfy the Gell-Mann–Oakes–Renner (GMOR) relation ([Gell-Mann, Oakes, and Renner, 1968](#))

$$m_P^2 f_P^2 = -m_q \langle \bar{\psi}\psi \rangle + \mathcal{O}(m_q^2) \quad (6)$$

with $f_\pi = \sqrt{2}F_\pi = 131$ MeV. The mass squared of the Goldstone bosons m_P^2 is in first order proportional to the mass of their valence quarks, [Eqs. \(5\) and \(6\)](#). This picture is the starting point of successful pion and kaon phenomenology.

A scalar confinement potential implies dynamical chiral symmetry breaking. For example, in the bag model of quark confinement is modeled by an infinite square well scalar potential. When quarks collide with the bag wall, their helicity is flipped. The bag wall thus connects left- and right-handed quarks leading to quark-pion coupling and the pion cloud of the nucleon ([Thomas, 1984](#)). Quark-pion coupling connected to chiral symmetry plays an important role in the proton's dynamics and phenomenology, e.g., transferring net quark spin into pion cloud orbital angular momentum and thus playing an important role in the nucleon's spin structure ([Bass and Thomas, 2010](#)).

¹Goldstone's theorem tells us that there is one massless pseudo-scalar boson for each symmetry generator that does not annihilate the vacuum.

TABLE I. The octet of Goldstone bosons corresponding to chiral SU(3) and their masses in free space.

Meson	Wave function	Mass (MeV)
π^0	$\frac{1}{\sqrt{2}}(u\bar{u} - d\bar{d})$	135
π^+	$u\bar{d}$	140
π^-	$\bar{u}d$	140
K^0	$d\bar{s}$	498
\bar{K}^0	$s\bar{d}$	498
K^+	$u\bar{s}$	494
K^-	$\bar{u}s$	494
η_8	$\frac{1}{\sqrt{6}}(u\bar{u} + d\bar{d} - 2s\bar{s})$	$\frac{4}{3}m_K^2 - \frac{1}{3}m_\pi^2$

The light-mass pion is especially important in nuclear physics, also with strong coupling to the lightest mass Δ p -wave nucleon resonance.

The QCD Hamiltonian is linear in the quark masses. For small quark masses this allows one to perform a rigorous expansion perturbing in $m_q \propto m_\pi^2$, called the chiral expansion (Gasser and Leutwyler, 1982). The proton mass in the chiral limit of massless quarks is determined by gluonic binding energy and set by Λ_{QCD} , which sets the scale for the running of the QCD coupling α_s , $\Lambda_{\text{QCD}} = 332 \pm 17$ MeV for QCD with three flavors (Patrignani *et al.*, 2016).

The lightest up and down quark masses are determined from detailed studies of chiral dynamics. One finds $m_u = 2.2^{+0.6}_{-0.4}$ MeV and $m_d = 4.7^{+0.5}_{-0.3}$ MeV whereas the strange-quark mass is slightly heavier at $m_s = 95 \pm 5$ MeV [with all values here quoted at the scale $\mu = 2$ GeV according to the Particle Data Group (Patrignani *et al.*, 2016)].

When electromagnetic interactions are also included, the leading-order mass relations Eq. (6) become (Georgi, 1984)

$$\begin{aligned}
 m_{\pi^\pm}^2 &= \mu(m_u + m_d) + \Delta m^2, \\
 m_{K^\pm}^2 &= \mu(m_u + m_s) + \Delta m^2, \\
 m_{K^0}^2 &= \mu(m_d + m_s), \\
 m_{\pi^0}^2 &= \mu(m_u + m_d), \\
 m_{\eta_8}^2 &= \mu(4m_s + m_u + m_d),
 \end{aligned} \tag{7}$$

where Δm^2 is the electromagnetic contribution (Dashen, 1969) and $\mu = -\langle \bar{\psi}\psi \rangle / f_\pi^2$. Substituting the pion and kaon masses gives the leading-order quark mass ratios

$$\left. \frac{m_s}{m_d} \right|_{\text{LO}} = 20, \quad \left. \frac{m_u}{m_d} \right|_{\text{LO}} = 0.55. \tag{8}$$

The leading-order GMOR formula (6) gives the Gell-Mann–Okubo formula (Gell-Mann, 1961; Okubo, 1962) for the octet state

$$4m_K^2 - m_\pi^2 = 3m_{\eta_8}^2. \tag{9}$$

Numerically $m_\eta(548 \text{ MeV}) \simeq m_{\eta_8}(570 \text{ MeV})$. The η meson mass and this η_8 mass contribution agree within 4% accuracy.

However, this is not the full story. The quark condensate in Eq. (6) also spontaneously breaks axial U(1) symmetry meaning that one might also expect a flavor-singlet

Goldstone state which mixes with the octet state to generate the isosinglet bosons. However, without extra input, the resultant bosons do not correspond to states in the physical spectrum. The lightest mass isosinglet bosons, the η and η' , are about 300–400 MeV too heavy to be pure Goldstone states, with masses $m_\eta = 548$ MeV and $m_{\eta'} = 958$ MeV. One needs extra mass in the flavor-singlet channel to connect to the physical η and η' mesons. This mass is associated with nonperturbative gluon dynamics.

The flavor-singlet channel is sensitive to processes involving violation of the Okubo-Zweig-Iizuka (OZI) rule, where the quark-antiquark pair (with quark chirality equal to 2) propagates with coupling to gluonic intermediate states (with zero net chirality); see Fig. 1. The OZI rule (Okubo, 1963; Zweig, 1964; Iizuka, 1966) is the phenomenological observation that hadronic processes involving Feynman graphs mediated by gluons (without continuous quark lines connecting the initial and final states) tend to be strongly suppressed.

To see the effect of the gluonic mass contribution consider the η - η' mass matrix for free mesons with rows and columns in the octet-singlet basis

$$\eta_8 = \frac{1}{\sqrt{6}}(u\bar{u} + d\bar{d} - 2s\bar{s}), \quad \eta_0 = \frac{1}{\sqrt{3}}(u\bar{u} + d\bar{d} + s\bar{s}). \tag{10}$$

At leading order in the chiral expansion (taking terms proportional to the quark masses m_q) this reads

$$M^2 = \begin{pmatrix} \frac{4}{3}m_K^2 - \frac{1}{3}m_\pi^2 & -\frac{2}{3}\sqrt{2}(m_K^2 - m_\pi^2) \\ -\frac{2}{3}\sqrt{2}(m_K^2 - m_\pi^2) & \left[\frac{2}{3}m_K^2 + \frac{1}{3}m_\pi^2 + \tilde{m}_{\eta_0}^2 \right] \end{pmatrix}. \tag{11}$$

Here $\tilde{m}_{\eta_0}^2$ is the flavor-singlet gluonic mass term.

In the notation of Eq. (7) these singlet and mixing terms are

$$\begin{aligned}
 m_{\eta_0}^2 &= \mu(m_u + m_d - 2m_s), \\
 \tilde{m}_{\eta_0}^2 &= \mu(m_u + m_d + m_s) + \tilde{m}_{\eta_0}^2.
 \end{aligned} \tag{12}$$

The masses of the physical η and η' mesons are found by diagonalizing this matrix, viz.,

$$\begin{aligned}
 |\eta\rangle &= \cos\theta|\eta_8\rangle - \sin\theta|\eta_0\rangle, \\
 |\eta'\rangle &= \sin\theta|\eta_8\rangle + \cos\theta|\eta_0\rangle.
 \end{aligned} \tag{13}$$

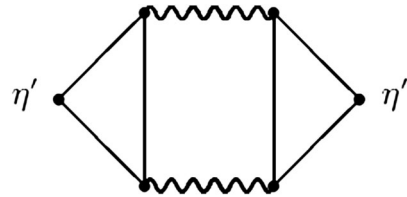


FIG. 1. Gluonic intermediate states contribute to the η' . The η' mixes a chirality-two quark-antiquark contribution and chirality-zero gluonic contribution.

One obtains the following values for the η and η' masses:

$$m_{\eta',\eta}^2 = (m_K^2 + \tilde{m}_{\eta_0}^2/2) \pm \frac{1}{2}\sqrt{(2m_K^2 - 2m_\pi^2 - \frac{1}{3}\tilde{m}_{\eta_0}^2)^2 + \frac{8}{9}\tilde{m}_{\eta_0}^4}. \quad (14)$$

Here the lightest mass state is η and the heavier state is η' . Summing over the two eigenvalues in Eq. (14) gives the Witten-Veneziano mass formula (Veneziano, 1979; Witten, 1979a)

$$m_\eta^2 + m_{\eta'}^2 = 2m_K^2 + \tilde{m}_{\eta_0}^2. \quad (15)$$

The gluonic mass term is obtained by substituting the physical values of m_η , $m_{\eta'}$, and m_K to give $\tilde{m}_{\eta_0}^2 = 0.73 \text{ GeV}^2$. Without the gluonic mass term η would be approximately an isosinglet light-quark state ($1/\sqrt{2}|\bar{u}u + \bar{d}d\rangle$) with mass $m_\eta \sim m_\pi$ degenerate with the pion and η' would be a strange-quark state $|\bar{s}s\rangle$ with mass $m_{\eta'} \sim \sqrt{2m_K^2 - m_\pi^2}$ —mirroring the isoscalar vector ω and ϕ mesons.

When interpreted in terms of the leading-order mixing scheme, Eq. (13), phenomenological studies of various decay processes give a value for the η - η' mixing angle between -15° and -20° (Gilman and Kauffman, 1987; Ball, Frere, and Tytgat, 1996; Ambrosino *et al.*, 2009). The η' has a large flavor-singlet component with strong affinity to couple to gluonic degrees of freedom. Mixing means that nonperturbative glue through axial U(1) dynamics plays an important role in both the η and η' and their interactions.

The gluonic mass term is associated with the QCD axial anomaly in the divergence of the flavor-singlet axial-vector current. While the nonsinglet axial-vector currents are partially conserved (they have just mass terms in the divergence), the singlet current $J_{\mu 5} = \bar{u}\gamma_\mu\gamma_5 u + \bar{d}\gamma_\mu\gamma_5 d + \bar{s}\gamma_\mu\gamma_5 s$ satisfies the divergence equation (Adler, 1969; Bell and Jackiw, 1969)

$$\partial^\mu J_{\mu 5} = 6Q + \sum_{k=1}^3 2im_k \bar{q}_k \gamma_5 q_k, \quad (16)$$

where

$$Q = \frac{\alpha_s}{8\pi} G_{\mu\nu} \tilde{G}^{\mu\nu}$$

is called the topological charge density. The anomalous gluonic term Q is induced by QCD quantum effects associated with renormalization of the singlet axial-vector current.² Here $G_{\mu\nu}$ is the gluon field tensor and $\tilde{G}^{\mu\nu} = (1/2)\epsilon^{\mu\nu\alpha\beta} G_{\alpha\beta}$. For reviews of anomaly physics, see Shifman (1989) and Ioffe

²In QCD the flavor-singlet axial-vector current can couple through gluon intermediate states; see Fig. 2. Here the triangle Feynman diagram is essential with the axial-vector current $\gamma_\mu\gamma_5$ and two gluon couplings γ_α and γ_β as the three vertices. When we regularize the ultraviolet behavior of momenta in the triangle loop, we find that we can preserve current conservation at the quark-gluon vertices (necessary for gauge invariance) or partial conservation of the axial-vector current but not both simultaneously. Current conservation wins and induces the gluonic anomaly term in the singlet divergence equation (16) from the ultraviolet pointlike part of the triangle loop.

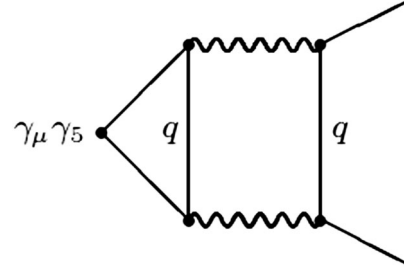


FIG. 2. Coupling of the axial-vector current through gluonic intermediate states. Gluon propagators are shown as wavy lines. Straight lines denote quark propagators.

(2006). Since gluons couple equally to each flavor of quark, the anomaly term cancels in the divergence equations for nonsinglet currents such as $J_{\mu 5}^{(3)} = \bar{u}\gamma_\mu\gamma_5 u - \bar{d}\gamma_\mu\gamma_5 d$ and $J_{\mu 5}^{(8)} = \bar{u}\gamma_\mu\gamma_5 u + \bar{d}\gamma_\mu\gamma_5 d - 2\bar{s}\gamma_\mu\gamma_5 s$.

The QCD anomaly means that the singlet current $J_{\mu 5}$ is not conserved for massless quarks. Nonperturbative gluon processes act to connect left- and right-handed quarks, whereas left- and right-handed massless quarks propagate independently in perturbative QCD with helicity conserved for massless quarks.

The integral over space $\int d^4z Q = n$ is quantized with either integer or fractional values and measures a property called the topological winding number. This winding number vanishes in perturbative QCD and in QED but is finite with nonperturbative glue, e.g., it is an integer for instantons (tunneling processes in the QCD vacuum that flip quark chirality) (Crewther, 1978).³ The gluonic mass term is generated by glue associated with this nontrivial topology, related perhaps to confinement or to instantons (Fritzsch and Minkowski, 1975; Kogut and Susskind, 1975; 't Hooft, 1976a, 1976b; Witten, 1979b). The exact details of this gluon dynamics are still debated.

It is interesting to consider QCD in the limit of a large number of colors $N_c \rightarrow \infty$. There are two well-defined theoretical limits taking $\alpha_s N_c$ and either N_f (the number of flavors) or N_f/N_c held fixed. The gluonic mass term has a rigorous interpretation as the leading term when one makes an expansion in $1/N_c$ in terms of a quantity $\chi(0)$ called the Yang-Mills topological susceptibility,

$$\tilde{m}_{\eta_0}^2|_{\text{LO}} = -\frac{6}{f_\pi^2} \chi(0)|_{\text{YM}}. \quad (17)$$

For an extended discussion, see Shore (1998, 2008). Here

$$\chi(k^2)|_{\text{YM}} = \int d^4z i e^{ik \cdot z} \langle \text{vac} | T Q(z) Q(0) | \text{vac} \rangle |_{\text{YM}} \quad (18)$$

³For a gluon field A_μ with gauge transformation \mathcal{G} , $A_\mu \rightarrow \mathcal{G}^{-1} A_\mu \mathcal{G} + (i/g) \mathcal{G}^{-1} (\partial_\mu \mathcal{G})$. Finite action requires that A_μ should tend to a pure gauge configuration when $x \rightarrow \infty$ with finite surface term integral $\int d^4x Q$ which takes quantized values, the topological winding number.

is calculated in the pure glue theory (without quarks). If we assume that the topological winding number remains finite independent of the value of N_c then $\tilde{m}_{\eta_0}^2 \sim 1/F_\pi^2 \sim 1/N_c$ as $N_c \rightarrow \infty$ (Witten, 1979a). In recent computational QCD lattice calculations Cichy *et al.* (2015) computed both the pure gluonic term on the right-hand side of Eq. (18) and the meson mass contributions with dynamical quarks in the Witten-Veneziano formula (15) and found excellent agreement at the 10% level. This calculation gives $\chi^{1/4}(0)|_{\text{YM}} = 185.3 \pm 5.6$ MeV, very close to the phenomenological value 180 MeV which follows from taking $\tilde{m}_{\eta_0}^2 = 0.73$ GeV² in the Witten-Veneziano formula (15).

Independent of the detailed QCD dynamics one can construct low-energy effective chiral Lagrangians which include the effect of the anomaly and axial U(1) symmetry (Di Vecchia and Veneziano, 1980; Kawarabayashi and Ohta, 1980; Rosenzweig, Schechter, and Trahern, 1980; Witten, 1980; Nath and Arnowitt, 1981; Leutwyler, 1998) and use these Lagrangians to study low-energy processes involving the η and η' . We define $U = e^{i(\phi/F_\pi + \sqrt{2/3}\eta_0/F_0)}$ as the unitary meson matrix where $\phi = \sum \pi_a \lambda_a$ denotes the octet of would-be Goldstone bosons π_a associated with spontaneous chiral symmetry breaking with λ_a as the Gell-Mann matrices [SU(3) generalizations of the isospin SU(2) Pauli matrices that couple to pions], η_0 is the singlet boson, and F_0 is the singlet decay constant (at leading order taken to be equal to $F_\pi = 92$ MeV). With this notation the kinetic energy and mass terms in the chiral Lagrangian are

$$\mathcal{L} = \frac{F_\pi^2}{4} \text{Tr}(\partial^\mu U \partial_\mu U^\dagger) + \frac{F_\pi^2}{4} \text{Tr} M(U + U^\dagger) \quad (19)$$

with M the meson mass matrix. The gluonic mass term $\tilde{m}_{\eta_0}^2$ is introduced via a flavor-singlet potential involving the topological charge density Q which is constructed so that the Lagrangian also reproduces the axial anomaly. This potential reads

$$\frac{1}{2} i Q \text{Tr}[\log U - \log U^\dagger] + \frac{3}{\tilde{m}_{\eta_0}^2 F_0^2} Q^2 \mapsto -\frac{1}{2} \tilde{m}_{\eta_0}^2 \eta_0^2, \quad (20)$$

where Q is eliminated through its equation of motion to give the gluonic mass term for the η' . The Lagrangian contains no kinetic energy term for Q , meaning that the gluonic potential does not correspond to a physical state; Q is therefore distinct from mixing with a pseudoscalar glueball state. The $Q\eta_0$ coupling in Eq. (20) reproduces the picture of the η' as a mixture of chirality ± 2 quark-antiquark and chirality-zero gluonic contributions; see Fig. 1.

Higher-order terms in Q^2 become important when we consider scattering processes involving more than one η' or η (Di Vecchia *et al.*, 1981); e.g., the term $Q^2 \partial_\mu \pi_a \partial^\mu \pi_a$ gives an OZI-violating tree-level contribution to the decay $\eta' \rightarrow \eta\pi\pi$. For the η' in a nuclear medium at finite density, the medium dependence of $\tilde{m}_{\eta_0}^2$ may be introduced through coupling to the σ mean field in the nucleus through the interaction term $\mathcal{L}_{\sigma Q} = g_{\sigma Q} Q^2 \sigma$. Here $g_{\sigma Q}$ denotes coupling to the σ field. Again eliminating Q through its equation of motion, one finds

the gluonic mass term decreases in-medium $\tilde{m}_{\eta_0}^{*2} < \tilde{m}_{\eta_0}^2$ independent of the sign of $g_{\sigma Q}$ and the medium acts to partially neutralize axial U(1) symmetry breaking by gluonic effects (Bass and Thomas, 2006). We return to this physics in Sec. VI. In general, couplings involving Q give OZI violation in physical observables.

Recent QCD lattice calculations suggest partial restoration of axial U(1) symmetry at finite temperature (Bazavov *et al.*, 2012; Cossu *et al.*, 2013; Tomiya *et al.*, 2017).

There are several places that glue enters η' and η meson physics: the gluon topology potential which generates the large η' mass, possible small mixing with a lightest mass pseudoscalar glueball state (which comes with a kinetic energy term in its Lagrangian) and, in high momentum transfer processes, radiatively generated glue associated with perturbative QCD. Possible candidates for the pseudoscalar glueball state are predicted by lattice QCD calculations with a mass above 2 GeV (Morningstar and Peardon, 1999; E. Gregory *et al.*, 2012; Sun *et al.*, 2017). These different gluonic contributions are distinct physics.

We have so far discussed the η and η' at leading order in the chiral expansion. Going beyond leading order, one becomes sensitive to extra SU(3) breaking through the difference in the pion and kaon decay constants $F_K = 1.22 F_\pi$ as well as new OZI-violating couplings. One finds strong mixing also in the decay constants. Two mixing angles enter the η - η' system when one extends the theory to $O(p^4)$ in the meson momentum (Leutwyler, 1998), viz.,

$$\begin{aligned} f_\eta^8 &= f_8 \cos \theta_8, & f_{\eta'}^8 &= f_8 \sin \theta_8, \\ f_\eta^0 &= -f_0 \sin \theta_0, & f_{\eta'}^0 &= f_0 \cos \theta_0. \end{aligned} \quad (21)$$

These mixing angles follow because the eigenstates of the mass matrix involve linear combinations of the different decay constants separated by SU(3) breaking multiplying the meson states. In the SU(3) symmetric world $F_\pi = F_K$ one would have $\theta_8 = \theta_0$, with both vanishing for massless quarks. One finds a systematic expansion, large N_c chiral perturbation theory, in $1/N_c = O(\delta)$, $p = O(\sqrt{\delta})$, and $m_q = O(\delta)$, where m_q are the light-quark masses and $\tilde{m}_{\eta_0}^2 \sim 1/N_c$.

Phenomenological fits have been made to production and decay processes within this two mixing angle scheme. The best fit values quoted by Feldmann (2000) are

$$\begin{aligned} f_8 &= (1.26 \pm 0.04) f_\pi, & \theta_8 &= -21.2^\circ \pm 1.6^\circ, \\ f_0 &= (1.17 \pm 0.03) f_\pi, & \theta_0 &= -9.2^\circ \pm 1.7^\circ, \end{aligned} \quad (22)$$

with the fits assuming that any extra OZI violation beyond $\tilde{m}_{\eta_0}^2$ can be turned off in first approximation. Similar numbers are obtained by Escribano and Frere (2005) and Shore (2006) and in recent QCD lattice calculations (Bali, Collins, and Simeth, 2018; Otnad and Urbach, 2018). To good approximation, this scheme reduces to one mixing angle if we change to the quark flavor basis $(1/\sqrt{2})(u\bar{u} + d\bar{d})$ and $s\bar{s}$, viz., $\phi = 39.3^\circ \pm 1^\circ$ (Feldmann, 2000). These numbers correspond to a mixing angle about -15° in the leading-order formula (13) (Feldmann, Kroll, and Stech, 1998).

Recent QCD lattice calculations give the following values for the mixing angles: $34^\circ \pm 3^\circ$ (E. B. Gregory *et al.*, 2012) and $46^\circ \pm 1^\circ \pm 3^\circ$ (Michael, Ottnad, and Urbach, 2013; Urbach, 2017) in the quark flavor basis and $-14.1^\circ \pm 2.8^\circ$ in the (leading-order) octet-singlet basis (Christ *et al.*, 2010).

Before discussing phenomenology, we first mention two key issues connected to the QCD anomaly which need to be kept in mind when understanding the η' . Observables do not depend on renormalization scales and are gauge invariant; that is, they do not depend on how a theoretician has set up a calculation.

First, the current $J_{\mu 5}$ picks up a dependence on the renormalization scale through the two-loop Feynman diagram in Fig. 2 (Crewther, 1978; Kodaira, 1980). This means that the singlet decay constant F_0 in QCD is sensitive to renormalization scale dependence. This is in contrast to F_π which is measured by the anomaly-free current $J_{\mu 5}^{(3)}$. A renormalization group (RG) scale invariant version of F_0 suitable for phenomenology can be defined by factoring out the scale dependence or, equivalently, taking the RG scale dependent quantity evaluated at $\mu^2 = \infty$. Numerically, the RG factor is about 0.84 if we take $\alpha_s(\mu_0^2) \sim 0.6$ as typical of the infrared region of QCD and evolve to infinity working to $\mathcal{O}(\alpha_s^2)$ in perturbative QCD (Bass, 2005).

Second, the topological charge density is a total divergence $Q = \partial^\mu K_\mu$. Here K_μ is the anomalous Chern-Simons current

$$K_\mu = \frac{g^2}{32\pi^2} \epsilon_{\mu\nu\rho\sigma} \left[A_a^\nu \left(\partial^\rho A_a^\sigma - \frac{1}{3} g f_{abc} A_b^\rho A_c^\sigma \right) \right] \quad (23)$$

with A_a^μ the gluon field and $\alpha_s = g^2/4\pi$ is the QCD coupling. The current K_μ is gauge dependent. Gauge dependence issues arise immediately if one tries to separate a “ K_μ contribution” from matrix elements of the singlet current $J_{\mu 5}$. This means that isolating the gluonic leading Fock component from the η' involves subtle issues of gauge invariance and makes sense only with respect to a particular renormalization scheme like the gauge invariant scheme $\overline{\text{MS}}$ (Bass, 2009).

III. THE STRONG CP PROBLEM AND AXIONS

The gluonic topology term (20) which generates the gluonic contribution to the η' mass also has the potential to induce strong CP violation in QCD. One finds an extra term $-\theta_{\text{QCD}} Q$ in the effective Lagrangian for axial U(1) physics which ensures that the potential

$$\frac{1}{2} i Q \text{Tr}[\log U - \log U^\dagger] + \frac{3}{\tilde{m}_{\eta_0}^2 F_0^2} Q^2 - \theta_{\text{QCD}} Q \quad (24)$$

is invariant under axial U(1) transformations with $U \rightarrow e^{-2i\alpha} U$ acting on the quark fields being compensated by $\theta_{\text{QCD}} \rightarrow \theta_{\text{QCD}} - 2\alpha N_f$.

The term $\theta_{\text{QCD}} Q$ is odd under CP symmetry. If it has nonzero value, θ_{QCD} induces a nonzero neutron electric dipole moment (Crewther *et al.*, 1979)

$$d_n = 5.2 \times 10^{-16} \theta_{\text{QCD}} e \text{ cm}. \quad (25)$$

Experiments constrain $|d_n| < 3.0 \times 10^{-26} e \text{ cm}$ at 90% confidence limit or $\theta_{\text{QCD}} < 10^{-10}$ (Pendlebury *et al.*, 2015). New and ongoing experiments aim for an order of magnitude improvement in precision within the next five years or so (Schmidt-Wellenburg, 2016).

Why is the strong CP violation parameter θ_{QCD} so small? QCD alone offers no answer to this question. QCD symmetries allow for a possible θ_{QCD} term but do not constrain its size. The value of θ_{QCD} is an external parameter in the theory just like the quark masses are.

Nonperturbative QCD arguments tell us that if the lightest quark had zero mass, then there would be no net CP violation connected to the θ_{QCD} term (Weinberg, 1996). However, chiral dynamics including the $\eta \rightarrow 3\pi$ decay discussed in Sec. IV.A tells us that the lightest up and down flavor quarks have small but finite masses. In the full standard model the parameter that determines the size of strong CP violation is $\Theta_{\text{QCD}} = \theta_{\text{QCD}} + \text{Arg det } \mathcal{M}_q$, where \mathcal{M}_q is the quark mass matrix. Possible strong CP violation then links QCD and the Higgs sector in the standard model that determines the quark masses.

A possible resolution of this strong CP puzzle is to postulate the existence of a new very-light mass pseudoscalar called the axion (Weinberg, 1978; Wilczek, 1978) which couples through the Lagrangian term

$$\mathcal{L}_a = -\frac{1}{2} \partial_\mu a \partial^\mu a + \left[\frac{a}{M} - \Theta_{\text{QCD}} \right] \frac{\alpha_s}{8\pi} G_{\mu\nu} \tilde{G}^{\mu\nu} + \frac{i f_\psi}{M} \partial_\mu a \bar{\psi} \gamma^\mu \gamma_5 \psi - \dots \quad (26)$$

Here the term in ψ denotes possible fermion couplings to the axion a . The mass scale M plays the role of the axion decay constant and sets the scale for this new physics. The axion transforms under a new global U(1) symmetry, called Peccei-Quinn symmetry (Peccei and Quinn, 1977), to cancel the Θ_{QCD} term, with strong CP violation replaced by the axion coupling to gluons and photons. The axion here develops a vacuum expectation value with the potential minimized at $\langle \text{vac} | a | \text{vac} \rangle / M = \Theta_{\text{QCD}}$. The mass of the QCD axion is given by (Weinberg, 1996)

$$m_a^2 = \frac{F_\pi^2}{M^2} \frac{m_u m_d}{(m_u + m_d)^2} m_\pi^2. \quad (27)$$

Axions are possible dark matter candidates. Constraints from experiments tell us that M must be very large. Laboratory experiments based on the two-photon anomalous couplings of the axion (Ringwald, 2015), ultracold neutron experiments to probe axion to gluon couplings (Abel *et al.*, 2017), together with astrophysics and cosmology constraints suggest a favored QCD axion mass between $1 \mu\text{eV}$ and 3 meV (Kawasaki and Nakayama, 2013; Baudis, 2018), which is the sensitivity range of the ADMX experiment in Seattle (Rosenberg, 2015), corresponding to M between about 6×10^9 and $6 \times 10^{12} \text{ GeV}$. The small axion interaction strength $\sim 1/M$ means that the small axion mass corresponds to a long lifetime and stable dark matter candidate, e.g., a lifetime longer than about the present age of the Universe. If

the axions were too heavy they would carry too much energy out of supernova explosions, thereby observably shortening the neutrino arrival pulse length recorded on Earth in contradiction to SN 1987a data (Kawasaki and Nakayama, 2013). Possible axion candidates would also need to be distinguished from other possible fifth force light-mass scalar bosons (Mantry, Pitschmann, and Ramsey-Musolf, 2014).

IV. η AND η' DECAYS

For the η and η' mesons there are two main decay types: hadronic decays to three pseudoscalar mesons and electromagnetic decays to two photons. The hadronic decays are sensitive to the details of chiral dynamics and, for decays into three pions, the difference in the light up and down quark masses. The two photon decays tell us about the spatial and quark or gluon structure of the mesons with extra (more model dependent) information coming from decays to η' final states (Rosner, 1983). Searches for rare and forbidden decays of the η and η' mesons constrain tests of fundamental symmetries.

The total widths quoted by the Particle Data Group are 1.31 ± 0.05 keV for the η meson and 0.196 ± 0.009 MeV for the η' meson (Patrignani *et al.*, 2016) with the η' result including the total width value determined directly from the mass distribution measured in proton-proton collisions, $\Gamma = 0.226 \pm 0.017 \pm 0.014$ MeV (Czerwinski *et al.*, 2010). The main branching ratios for the η decays are $\eta \rightarrow 3\pi^0$ at $32.68\% \pm 0.23\%$, $\eta \rightarrow \pi^+\pi^-\pi^0$ at $22.92\% \pm 0.28\%$, and $39.31\% \pm 0.20\%$ for the two-photon decay $\eta \rightarrow 2\gamma$. For η' the main decays are $\eta' \rightarrow \eta\pi^+\pi^-$ at $42.6\% \pm 0.7\%$ and $\eta' \rightarrow \eta\pi^0\pi^0$ at $22.8\% \pm 0.8\%$ (Patrignani *et al.*, 2016).

A. Hadronic decays

The $\eta \rightarrow 3\pi$ decay is of key interest. This process is driven by isospin violation in the QCD Lagrangian, the difference in light-quark up and down quark masses $m_u \neq m_d$. In the absence of small (few percent) electromagnetic contributions (Baur, Kambor, and Wyler, 1996), the decay amplitude is proportional to $m_d - m_u$ which is usually expressed in terms of the ratio

$$\frac{1}{R_m^2} = \frac{m_d^2 - m_u^2}{m_s^2 - \hat{m}^2}, \quad (28)$$

where $\hat{m} = (1/2)(m_d + m_u)$ and m_s is the strange quark mass. Expansion in chiral perturbation theory (in the light-quark masses) converges slowly due to final state pion rescattering effects. Fortunately, these can be resummed using dispersive techniques allowing one to make a precise determination of the ratio of light-quark masses from experiments; for a review see Leutwyler (2013).

Recent accurate measurements of the η decay to charged pions $\eta \rightarrow \pi^+\pi^-\pi^0$ have been performed by the WASA-at-COSY experiment at FZ-Jülich (Adlarson *et al.*, 2014b), the KLOE-2 Collaboration at LN-Frascati (Anastasi *et al.*, 2016), and at BES in Beijing (Ablikim *et al.*, 2017). The neutral three pion decay $\eta \rightarrow 3\pi^0$ has most recently been measured by WASA (Adolph *et al.*, 2009), KLOE (Ambrosino *et al.*, 2010),

the Mainz A2 Collaboration (Prakhov *et al.*, 2018), and at BES (Ablikim *et al.*, 2015a).

Taking the precise data on $\eta \rightarrow \pi^+\pi^-\pi^0$ from KLOE-2 as input, Colangelo *et al.* (2017) found $R_m = 22.0 \pm 0.7$. Combining this result with $m_s/\hat{m} = 27.30(34)$ quoted in the lattice reference (Aoki *et al.*, 2017), they obtained the light-quark mass ratio $m_u/m_d = 0.44(3)$. Similar results have been obtained by Guo *et al.* (2017) who include both KLOE-2 and WASA data for this decay and get $R_m = 21.6 \pm 1.1$. Similar values for R_m were found using earlier data by Kambor, Wiesendanger, and Wyler (1996) and Kampf *et al.* (2011). These numbers compare with $R_m = 23.9$ which follows from the simple leading-order calculation in Eq. (8).

The decay $\eta' \rightarrow 3\pi$ is also driven by isospin violation. In addition to the QCD processes involved in the η decay, here there are also important contributions from the subprocesses $\eta' \rightarrow \eta\pi\pi$ plus $\eta\pi^0$ mixing to give the three pion final state and $\eta' \rightarrow \pi\rho$ with $\rho \rightarrow \pi\pi$.

These decays contrast with the process $\eta' \rightarrow \eta\pi\pi$ which is the dominant η' decay with leading QCD term not driven by the difference in m_u and m_d . Here the singlet component in both the initial and final state isoscalar mesons η' and η through η - η' mixing means that the reaction is potentially sensitive also to OZI-violating couplings, e.g., from the $Q^2\partial^\mu\pi_a\partial_\mu\pi_a$ term at next-to-leading order in $1/N_c$ in the chiral Lagrangian. The leading-order amplitude for this decay is proportional to m_π^2 and vanishes in the chiral limit. The large branching ratios for this decay tell us that nonleading terms play a vital role.

We refer to Kupsc (2009) for further details of the analysis of these processes and to Fang, Kupsc, and Wei (2018) for a review of the latest experimental results from the BES experiment, as well as earlier measurements of these decays.

B. Two-photon interactions

The two-photon decays of the π^0 , η , and η' mesons are driven by the QED axial anomaly.

For the π^0 , in the chiral limit

$$F_\pi g_{\pi^0\gamma\gamma} = \frac{N_c}{3\pi} \alpha, \quad (29)$$

where $g_{\pi^0\gamma\gamma}$ is the π^0 two-photon coupling, N_c is the number of colors ($= 3$), and α is the electromagnetic coupling. Without the QED anomaly the decay amplitude would be proportional to m_π^2 and vanish for massless quarks.

For the isoscalar mesons one also has to consider the QCD gluon axial anomaly. In the chiral limit one finds (Shore and Veneziano, 1992)

$$F_0 \left[g_{\eta'\gamma\gamma} + \frac{1}{N_f} F_0 m_{\eta'}^2 g_{Q\gamma\gamma}(0) \right] = \frac{4N_c}{3\pi} \alpha. \quad (30)$$

Here $g_{\eta'\gamma\gamma}$ and $g_{Q\gamma\gamma}$ denote the two-photon couplings of the physical η' and topological charge density term. Chiral corrections have been discussed by Shore (2006) within the context of the two mixing angle scheme. The observed decay

rates for η and η' suggest small gluonic coupling $g_{Q\gamma\gamma} \sim 0$ with the gluonic term contributing at most 10% of the η' decay (Shore, 2006). Most accurate measurements of the $\eta \rightarrow \gamma\gamma$ and $\eta' \rightarrow \gamma\gamma$ decays come from KLOE-2 (Babusci *et al.*, 2013a) and BELLE (Adachi *et al.*, 2008), respectively.

When one or both of the photons become virtual, the pseudoscalar meson coupling to two-photon amplitudes involves transition form factors $F_{P\gamma}(q^2)$ associated with the spatial structure of the mesons.

There are measurements in both spacelike $Q^2 = -q^2 > 0$ and timelike $q^2 > 0$ kinematics where q is the four-momentum transfer in the reaction.⁴ The spacelike region can be studied through $\gamma\gamma^* \rightarrow P$ fusion processes in electron-positron collisions, with η and η' production data from CELLO (Behrend *et al.*, 1991), CLEO (Gronberg *et al.*, 1998), BABAR (del Amo Sanchez *et al.*, 2011), and KLOE-2 (Babusci *et al.*, 2013a). The timelike region is studied in meson decays $P \rightarrow \gamma\gamma^*$, $\gamma^* \rightarrow l^+l^-$, e.g., Dalitz decays to lepton pairs in the final state with positive q^2 equal to the invariant mass of the final state lepton pair l^+l^- . Single and double Dalitz decays can be studied. Recent measurements for the η come from the A2 Collaboration at Mainz (Adlarson *et al.*, 2017a), WASA-at-COSY (Adlarson *et al.*, 2016), and NA60 at CERN (Arnaldi *et al.*, 2009), with data from BES-III (Ablikim *et al.*, 2015b) for the η' .

Production of a pseudoscalar meson P through fusion of a real and deeply virtual photon $\gamma\gamma^* \rightarrow P$ is described by perturbative QCD in terms of light-front wave functions (Lepage and Brodsky, 1980; Feldmann and Kroll, 1998). In the asymptotic large Q^2 limit, the transition form factors for $\gamma\gamma^* \rightarrow P$

$$Q^2 F_{P\gamma}(Q^2) \rightarrow 6 \sum_a C_a f_P^a \quad (Q^2 \rightarrow \infty). \quad (31)$$

Here mixing is encoded in the decay constants f_P^a and C_a are the quark charge factors. The light-cone wave functions $\Psi_P^a(x, \vec{k}_t)$ describe the amplitude for finding a quark-antiquark pair carrying light-cone momentum fraction x and $1-x$ and transverse momentum \vec{k}_t . These amplitudes are normalized via

$$\int \frac{d^2\vec{k}_t}{16\pi^3} \int_0^1 dx \Psi_P^a(x, \vec{k}_t) = \frac{f_P^a}{2\sqrt{6}}. \quad (32)$$

As explained in Sec. II, one cannot separate an anomalous K_μ contribution from F_0 when working with gauge invariant observables, e.g., using $\overline{\text{MS}}$ renormalization. The small OZI violation in F_0 is consistent with RG effects and with the quark-antiquark leading Fock component moving in a topological gluon potential. Glue may be strongly excited in the intermediate states of hadronic reactions.

⁴Here Q^2 denotes the squared four-momentum transfer of the virtual photon and should not be confused with “ Q ” in our previous discussion where it denoted the topological charge density. For consistency with the literature we keep Q here for both cases.

The low q^2 region is described using form factors

$$F(q^2) = F(0) \frac{\Lambda^2}{\Lambda^2 - q^2 - i\Gamma\Lambda}. \quad (33)$$

The slope parameter

$$b_P = \left. \frac{d|F(q^2)|}{dq^2} \right|_{q^2=0} = F(0) \frac{1}{\Lambda^2 + \Gamma^2} \quad (34)$$

is often quoted for the decays. Values extracted for the η' from timelike decays are $b_{\eta'} = 1.60 \pm 0.17 \pm 0.08 \text{ GeV}^{-2}$ and $\Lambda = 0.79 \pm 0.04 \pm 0.02 \text{ GeV}$ from BES-III (Ablikim *et al.*, 2015b), with Λ close to the ω and ρ masses which appear with vector meson dominance of the virtual photon. In the spacelike region the CELLO Collaboration found $b_{\eta'} = 1.60 \pm 0.16 \text{ GeV}^{-2}$ (Behrend *et al.*, 1991). Note that the Γ width term is important here for the η' because of its large mass and short lifetime. For the η slope measured in timelike decays, the most precise measurement of Λ_{η}^{-2} is $1.97 \pm 0.11 \text{ GeV}^{-2}$ from the A2 Collaboration at Mainz (Adlarson *et al.*, 2017a).

Extending the final states from charged leptons to charged pions, the process $\eta \rightarrow \pi^+\pi^-\gamma$ includes contributions from both the transition form factor and the box anomaly shown in Fig. 3. Recent measurements are from WASA (Adlarson *et al.*, 2012) and KLOE-2 (Babusci *et al.*, 2013b). For a recent theoretical discussion see Kubis and Plenter (2015).

The $\eta'\gamma$ transition form factor for deeply virtual $\gamma^*\gamma \rightarrow \eta'$ was interpreted by Kroll and Passek-Kumericki (2013) to give a quite large (radiatively generated) two gluon Fock component in the η' wave function. In this calculation the glue enters at next-to-leading order. Exclusive central production of η' in high-energy proton-proton collisions at the LHC has been suggested as a cleaner probe since here the glue enters at leading order (Harland-Lang *et al.*, 2013).

In lower energy experiments, quark model inspired fits including a “gluonium admixture” (Rosner, 1983) have been performed to various low-energy processes including the $\phi \rightarrow \eta'\gamma$ decay by the KLOE Collaboration (Ambrosino *et al.*, 2007, 2009; Gauzzi, 2012) suggesting a phenomenological “gluonium fraction” of 0.12 ± 0.04 . Various theoretical groups’ analyses of the same data suggest values between zero and about 10% depending on form factors that are used in the fits (Escribano and Nadal, 2007; Thomas, 2007; Di Donato, Ricciardi, and Bigi, 2012). When trying to extract a “gluonic content” from experiments it is important to be careful what assumptions about glue have gone into the analyses. Photon coupling decay processes are theoretically cleaner with less model dependence in their interpretation.

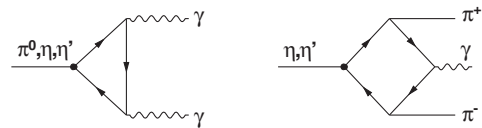


FIG. 3. Feynman diagrams for the triangle and box anomalies. The anomaly comes from the pointlike part of the quark loop with the quarks carrying maximum momentum in the loop.

At high energies, heavy-quark meson decays to light-quark states including the η' proceed through OZI-violating gluonic intermediate states, e.g., J/Ψ to $\eta'\gamma$ and $\eta\gamma$ giving experimental constraints on the flavor-singlet components in these mesons. In high-energy processes large branching ratios for D_s and B meson decays to η' final states have been observed and are believed to be driven in part by coupling to gluonic intermediate states (Ball, Frere, and Tytgat, 1996; Dighe, Gronau, and Rosner, 1996, 1997; Atwood and Soni, 1997; Fritzsche, 1997; Behrens *et al.*, 1998; Browder *et al.*, 1998; Hou and Tseng, 1998; Aubert *et al.*, 2001; Bali *et al.*, 2015).

C. Precision tests of fundamental symmetries

Precision measurements of the muon's anomalous magnetic moment $a_\mu = (g - 2)/2$ are an important test of the standard model. The anomalous magnetic moment is induced by quantum radiative corrections to the magnetic moment with g the proportionality constant between the particle's magnetic moment and its spin. The present experimental value from BNL (Bennett *et al.*, 2006)

$$a_\mu^{\text{exp}} = (11\,659\,209.1 \pm 5.4 \pm 3.3) \times 10^{-10} \quad (35)$$

differs from the present best theoretical expectation by

$$a_\mu^{\text{exp}} - a_\mu^{\text{th}} = (31.3 \pm 7.7) \times 10^{-10}, \quad (36)$$

a 4.1σ deviation (Jegerlehner, 2017). This result is also a puzzle since possible new physics contributions which might have resolved the discrepancy are now seriously challenged by LHC data which are, so far, consistent with the standard model and no extra new particles in the mass range of the experiments. New experiments at Fermilab and J-PARC plan to check this result with the Fermilab experiment improving the present statistical error on a_μ from 540 to 140 ppb or 1.4×10^{-10} (Hertzog, 2016).

One key issue is the size of low-energy QCD hadronic contributions to the muon $g - 2$. These are the biggest source of theoretical uncertainty in the standard model prediction with one important ingredient being the hadronic contributions to virtual photon-photon scattering with meson intermediate states. These are sensitive to the π^0 , η , and η' transition form factors. Various calculations appear in the literature; see Table 5.13, p. 474, in Jegerlehner (2017). Contributions to a_μ from the η and η' are typically about 3×10^{-10} with pion contributions between about 5×10^{-10} and 8×10^{-10} . The total hadronic contribution to a_μ including vacuum polarization effects is about 690×10^{-10} with a net light-by-light contribution of about 10×10^{-10} after summing over terms with positive and negative signs.

Studies of η meson decays also provide new precision tests of discrete symmetries: charge conjugation C and charge parity CP (Jarlskog and Shabalin, 2002). The η and η' mesons are eigenstates of parity P , charge conjugation, and combined CP parity with eigenvalues $P = -1$, $C = +1$, and $CP = -1$. C tests include searches for forbidden decays to an odd number of photons, e.g., $\eta \rightarrow 3\gamma$ (Nefkens *et al.*, 2005a), $\eta \rightarrow \pi^0\gamma$ (which is also forbidden by angular momentum

conservation) (Adlarson *et al.*, 2018a), and $\eta \rightarrow 2\pi^0\gamma$ (Nefkens *et al.*, 2005b). Charge conjugation invariance has also been tested in the $\eta \rightarrow \pi^0\pi^+\pi^-$ decay. Here C violation can manifest itself as an asymmetry in the energy distributions for π^+ and π^- mesons in the rest frame of the η meson. The results were found consistent with zero (Adlarson *et al.*, 2014b). A possible CP violating asymmetry in the $\eta \rightarrow \pi^+\pi^-e^+e^-$ decay was determined consistent with zero (Adlarson *et al.*, 2016).

V. η - AND η' -NUCLEON INTERACTIONS

Close-to-threshold η and η' production is studied in photon-nucleon and proton-nucleon collisions. Photon induced reactions are important for studies of nucleon resonance excitations; for a recent review, see Krusche and Wilkin (2015). η meson production is characterized by the strong role of the s -wave $N^*(1535)$ resonance. For studies of higher mass excited resonances, recent advances with double polarization observables are playing a vital role. Recent measurements for the η come from Mainz (Witthauer *et al.*, 2016, 2017), Jefferson Laboratory (Senderovich *et al.*, 2016; Al Ghoul *et al.*, 2017), and GrAAL (Levi Sandri *et al.*, 2015), with partial-wave analysis studies reported by Anisovich *et al.* (2015).

For the η' (quasifree) photoproduction from proton and deuteron targets has been studied at ELSA (Crede *et al.*, 2009; Jaegle *et al.*, 2011; Krusche, 2012), MAMI (Kashevarov *et al.*, 2017), and by the CLAS experiment at Jefferson Laboratory (Dugger *et al.*, 2006; Williams *et al.*, 2009) with new double polarization observables reported by Collins *et al.* (2017). The production cross section is isospin independent for incident photon energies greater than 2 GeV, where t -channel exchanges are important. At lower energies, particularly between 1.6 and 1.9 GeV where the proton cross section peaks, the proton and quasifree neutron cross sections show different behavior. These data have recently been used in partial-wave analysis revealing strong indications of four excited nucleon resonances contributing to the η' production process: $N(1895)_{\frac{1}{2}}^-$, $N(1900)_{\frac{3}{2}}^+$, $N(2100)_{\frac{1}{2}}^+$, and $N(2120)_{\frac{3}{2}}^-$. Details including the branching ratios for coupling to the η' are given by Anisovich *et al.* (2017).

In proton-nucleon collisions the η and η' production processes proceed through exchange of a complete set of virtual meson hadronic states, which in models is usually truncated to single virtual meson exchange, e.g., π , η , ρ , ω , and σ (correlated two-pion) exchanges (Fäldt and Wilkin, 2001; Pena, Garcilazo, and Riska, 2001; Nakayama *et al.*, 2003; Deloff, 2004; Shyam, 2007). For the η' OZI-violating production is also possible through excitation of nonperturbative glue in the interaction region (Bass, 1999). The exchange process can also induce nucleon resonance excitation, especially the $N^*(1535)$ with η production, before final emission of the η or η' meson. The production mechanism is studied through measurements of the total and differential cross sections, varying the isospin of the second nucleon and polarization observables with one of the incident protons transversely polarized (Moskal, 2004). The interpretation of these processes is sensitive to the choice of exchanged mesons and nucleon resonances included in the models and the

truncation of the virtual exchange contributions which affects, e.g., the meson-nucleon form factors in the calculations.

The near-threshold η meson production in nucleon-nucleon collisions has been investigated extensively at the CELSIUS, COSY, and SATURNE facilities. The results determined by different experiments for the total cross sections (Bergdolt *et al.*, 1993; Chiavassa *et al.*, 1994; Calen *et al.*, 1996; Hibou *et al.*, 1998; Smyrski *et al.*, 2000; Moskal *et al.*, 2004, 2010) and different cross sections (Abdel-Bary *et al.*, 2003; Moskal *et al.*, 2004, 2010; Petren *et al.*, 2010) for the $pp \rightarrow pp\eta$ reaction and for the quasifree $pn \rightarrow pn\eta$ reaction (Calen *et al.*, 1996, 1998; Moskal *et al.*, 2009) are consistent within the estimated uncertainties. In the different experiments η mesons could be produced up to excess energy \mathcal{E} of 92 MeV at CELSIUS, 502 MeV at COSY, and 593 MeV at SATURNE.

η' production has been measured in proton-proton collisions close to threshold (excess energy \mathcal{E} between 0.76 and ~ 50 MeV) by the COSY-11 Collaboration at FZ-Jülich (Moskal *et al.*, 1998, 2000a, 2000b; Khoukaz *et al.*, 2004; Klaja *et al.*, 2010b; Czerwinski, Moskal, and Silarski, 2014) and at $\mathcal{E} = 3.7$ and 8.3 MeV by SPESIII (Hibou *et al.*, 1998) and 144 MeV by the DISTO Collaboration at SATURNE (Balestra *et al.*, 2000).

For near-threshold meson production, the cross section is reduced by initial state interaction between the incident nucleons and enhanced by final state interactions between the outgoing hadrons. For comparing production dynamics a natural variable is the volume of available phase space which is approximately independent of the meson mass. Making this comparison for the neutral pseudoscalar mesons, it was found that production of the η meson is about 6 times enhanced compared to the π^0 which is 6 times further enhanced compared to the η' . The production amplitudes for π^0 and η' have the same (nearly constant) dependence on the phase space volume in the measured kinematics close to threshold, whereas the production amplitude for η exhibits possible growth with decreasing phase space volume due to strong η -proton attractive interaction (Moskal *et al.*, 2000b). The large η production cross section is driven by strong coupling to $N^*(1535)$. In Fig. 4 we show the η and η' production total cross-section data as a function of excess energy. Figure 4 also shows the curves expected if one includes only the s wave and final state interaction in the proton-proton in the simplest approximation (Fäldt and Wilkin, 1996; Wilkin, 2016):

$$\sigma_T(pp \rightarrow pp\eta) = C \left(\frac{\mathcal{E}}{\mu} \right)^2 \left/ \left(1 + \sqrt{1 + \mathcal{E}/\mu} \right)^2 \right. \quad (37)$$

Here the excess energy $\mathcal{E} = W - (2m_p + m)$, with W the total center-of-mass energy, m_p the proton mass, and m the meson mass. The constant C depends upon the reaction mechanism and can be adjusted to fit the data. Strong η -nucleon final state interaction is seen at the lowest \mathcal{E} with deviation of the data from the theoretical curve, much stronger than for the η' . Deviations at large \mathcal{E} are likely to originate from higher partial waves in the final proton-proton system. The pole parameter μ fitted from experiment is ≈ 0.75 MeV for the η' (Wilkin, 2016).

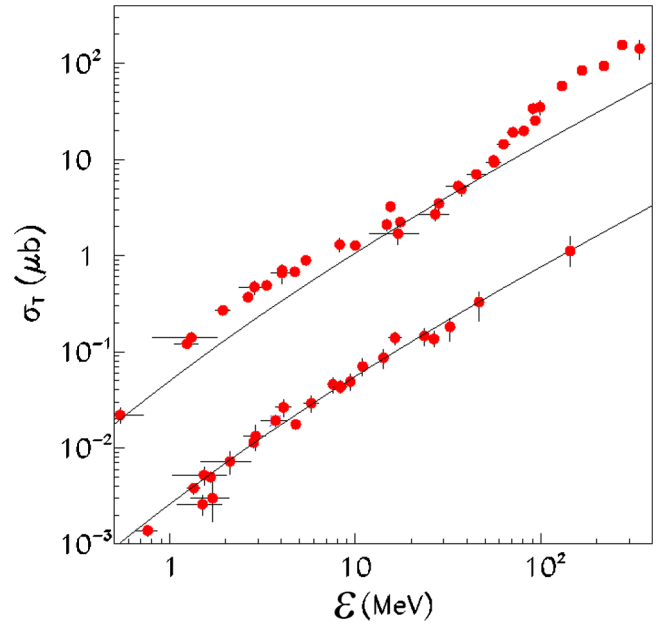


FIG. 4. World data for the total cross sections for $pp \rightarrow pp\eta$ (upper points) and $pp \rightarrow pp\eta'$ (lower points); see the text. The solid curves are arbitrarily scaled pp FSI predictions of Eq. (37). Adapted from Wilkin, 2016.

Measurements of the differential cross sections for η production at $\mathcal{E} = 15.5$ MeV (Moskal *et al.*, 2004) and at $\mathcal{E} = 41$ MeV (Abdel-Bary *et al.*, 2003) are consistent with isotropic η production within the statistical errors, although at 41 MeV the accuracy of the data does not exclude a few percent contribution from higher partial waves. For η' production, the differential cross sections measured at SATURNE (Balestra *et al.*, 2000) at $\mathcal{E} = 143.8$ MeV and at COSY (Khoukaz *et al.*, 2004) at $\mathcal{E} = 46.6$ MeV are consistent with pure Ss -wave production with $\approx 10\%$ level higher partial-wave contributions possible within the experimental uncertainties. Here Ss denotes the outgoing protons in S wave in their rest frame and the meson is in s wave relative to the center of mass.

Values for the real part of the η -nucleon scattering length $a_{\eta N}$ have been obtained between 0.2 and 1.05 fm depending on the analysis, including whether the η - η' mixing angle is constrained or not. Fits to experimental data suggest a value close to 0.9 fm for the real part of $a_{\eta N}$ (Green and Wycech, 1999, 2005; Arndt *et al.*, 2005). In contrast, smaller values of $a_{\eta N}$ with real part ~ 0.2 fm are predicted by chiral coupled-channel models where the η meson is treated in pure octet approximation (Waas and Weise, 1997; Garcia-Recio *et al.*, 2002; Inoue and Oset, 2002).

The scattering length $a_{\eta N}$ is much greater than the scattering length for pion-nucleon scattering. Pion-nucleon interactions are dominated by the p -wave Δ (lightest mass) nucleon resonance excitation with small scattering length, which for the π^0 the real part is $a_{\pi N} = 0.1294 \pm 0.0009$ fm (Sigg *et al.*, 1996).

The COSY-11 Collaboration have recently made a first measurement of the η' -nucleon scattering length in free space,

$$a_{\eta' p} = (0 \pm 0.43) + i(0.37^{+0.40}_{-0.16}) \text{ fm} \quad (38)$$

from studies of the η' final state interaction in η' production in proton-proton collisions close to threshold (Czerwinski *et al.*, 2014). This value was extracted from fitting the low \mathcal{E} data, \mathcal{E} up to 11 MeV, where the cross section is clearly s -wave dominated. A recent extraction from photoproduction data gives

$$|a_{\eta'N}| = 0.403 \pm 0.015 \pm 0.060 \text{ fm} \quad (39)$$

with phase $87^\circ \pm 2^\circ$ (Anisovich *et al.*, 2018). Theoretical models in general prefer a positive sign for the real part of $a_{\eta'p}$ corresponding to attractive interaction. The meson-nucleon scattering lengths are also related to the corresponding meson-nucleus optical potential; see Sec. VI. Measurements of the η' mass shift in carbon favor a value for the real part of $a_{\eta'N}$ of about 0.5 fm.

These numbers can be understood in terms of the underlying dynamics. In chiral dynamics, the Goldstone-boson nucleon scattering lengths are proportional at tree level to the meson mass squared, e.g., the Tomozawa-Weinberg relation (Ericson and Weise, 1988). For pion-nucleon scattering, the nearest s -wave resonance is the $N^*(1535)$, which is too far away to affect the near-threshold interaction. For the η one finds a strong effect from the close-to-threshold resonance $N^*(1535)$. With the η' , the meson mass squared is large through the gluonic mass term $\tilde{m}_{\eta_0}^2$. The tree-level scattering length is nonvanishing in the chiral limit.

Measurements of the isospin dependence of η meson production in proton-nucleon collisions revealed that the total cross section for the quasifree $pn \rightarrow pn\eta$ reaction exceeds the corresponding cross section for $pp \rightarrow pp\eta$ by a factor of about 3 at threshold and by a factor of 6 at higher excess energies between about 25 and 100 MeV (Calen *et al.*, 1998; Moskal *et al.*, 2009). The strong isospin dependence tells us there must be a significant isovector exchange contribution at work in the proton-nucleon collisions.

The spin analyzing power A_y for η meson production in proton-proton collisions close to threshold with one proton beam transversely polarized has recently been measured with high statistics by the WASA-at-COSY Collaboration (Adlarson *et al.*, 2018b). The analyzing power is found to be consistent with zero for an excess energy of $\mathcal{E} = 15$ MeV signaling s wave production with no evidence for higher partial waves. This result is in contrast with meson-exchange model predictions which had anticipated asymmetries up to about 20% based on π or ρ exchange dominance in the interaction (Fäldt and Wilkin, 2001; Nakayama *et al.*, 2003); see Fig. 5. At $\mathcal{E} = 72$ MeV the data reveal strong interference of Ps and Pp partial waves and cancellation of $(Pp)^2$ and Ss^*Sd contributions (Adlarson *et al.*, 2018b). Different meson exchanges induce very different spin dependence in the production process. Polarized beams and measurement of the analyzing power can therefore put powerful new constraints on theoretical understanding of the η production process. A possible explanation of the vanishing analyzing power at 15 MeV might be cancellation with destructive interference between π and ρ exchanges in η production very close to threshold together with a strong (spin independent) scalar σ (correlated two pion) exchange contribution. In this

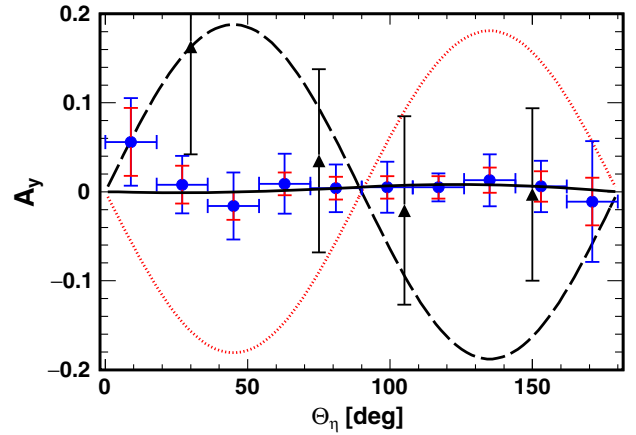


FIG. 5. Analyzing power for the $\bar{p}p \rightarrow pp\eta$ reaction at $Q = 15$ MeV. Here θ_η is the polar angle for the emission of the η meson in the center-of-mass system. Full circles represent WASA results (Adlarson *et al.*, 2018b). Triangles are early data from COSY-11 measured at $\mathcal{E} = 10$ MeV (Czyzykiewicz *et al.*, 2007). The dotted line denotes the prediction based on pseudo-scalar-meson exchange (Nakayama *et al.*, 2003), whereas the dashed line represents the vector exchange model (Fäldt and Wilkin, 2001). The solid line is the partial-waves fit to the WASA data. Adapted from Adlarson *et al.*, 2018b.

scenario one would expect to see a finite analyzing power in proton-neutron collisions given the strong isospin dependence to the production mechanism.

Measurements of the isospin dependence of η' production suggest a different production mechanism for this meson (Moskal *et al.*, 2000b; Klaja *et al.*, 2010a). Using the quasifree proton-neutron interaction (Moskal *et al.*, 2006) COSY-11 placed an upper bound on $\sigma(pn \rightarrow pn\eta')$ and the ratio $R_{\eta'} = \sigma(pn \rightarrow pn\eta')/\sigma(pp \rightarrow pp\eta')$ (Klaja *et al.*, 2010a). For excess energy between 8 and 24 MeV the upper limit of $R_{\eta'}$ was observed to be consistently 1 standard deviation below the corresponding ratio for η production (Moskal *et al.*, 2009). In the theoretical limit that η' production proceeds entirely through gluonic excitation in the intermediate state this ratio would go to 1. The data are consistent with both a role for OZI-violating η' production (Bass, 1999, 2000) and the meson-exchange model (Kaptari and Kampf, 2008).

The observed s -wave dominance of η and η' production in a large kinematic range close to threshold might also, in part, be understood in terms of the phenomenology of Gell-Mann and Watson (1954). If the strength of the primary production partial amplitudes were constant over the phase space, then the energy dependence of the partial cross sections would be given by

$$\sigma_{LI} \propto q_{\max}^{2L+2I+4} \propto \eta_M^{2L+2I+4}. \quad (40)$$

Here $\eta_M = q_{\max}/m$ with m and q_{\max} the mass and maximum momentum of the created meson. Close to threshold the Ss partial-wave cross section should increase with the fourth power of η_M which, nonrelativistically, is related to the excess energy by $\mathcal{E} = \eta_M^2 m(2m_p + m)/4m_p$. The orbital angular momentum l of the produced meson is $l = Rq \sim q/m$, where

R is a characteristic distance from the center of the collision $R \sim 1/m \sim 1/\Delta p$ with m the meson mass and Δp the momentum transfer between the colliding nucleons. Hence η_M denotes the classically calculated maximum angular momentum of the meson in the center-of-mass frame.

Investigations with polarized beams and targets (Meyer *et al.*, 1999, 2001) of the $\vec{p}\vec{p} \rightarrow pp\pi^0$ reaction tell us that the Ss partial wave accounts for more than 95% of the total cross section up to $\eta_M \approx 0.4$. Extending this phenomenology to heavy mesons suggests that the Ss partial-wave combination will constitute the overwhelming fraction of the total production cross section for η_M smaller than about 0.4 for constant production amplitudes $|M_{LL}^0|$. That is, one expects the heavier η and η' mesons to be produced predominantly via the Ss state in a much larger excess energy range and hence larger phase space volume. Whereas for π^0 production the onset of higher partial waves is observed at \mathcal{E} around 10 MeV, it is expected only above 100 MeV for the η' and above ≈ 40 MeV for the η meson (modulo the possible small change in amplitude with increasing phase space volume) (Moskal *et al.*, 2000b; Klaja *et al.*, 2010b).

A. The $N^*(1535)$ resonance and its structure

The internal structure of the $N^*(1535)$ has been a hot topic of discussion. In quark models the $N^*(1535)$ is interpreted as a three-quark state: $(1s)^2(1p)$. One finds configuration mixing with the $N^*(1650)$ between $|^2P_{1/2}\rangle$ and $|^4P_{1/2}\rangle$ states (with spin 1/2 and 3/2, respectively, orbital angular momentum $L = 1$ and total angular momentum $J = 1/2$) (Isgur and Karl, 1978). Recent QCD lattice calculations support a three-quark state, with couplings to five quark components and probability of about 50% to contain the bare baryon (Liu *et al.*, 2016). This contrasts with the $\Lambda(1405)$ resonance which is understood as dynamically generated in the kaon-nucleon system (Hall *et al.*, 2015). The structure of the $N^*(1535)$ has also been discussed within chiral coupled-channel models (Kaiser, Siegel, and Weise, 1995; Inoue, Oset, and Vicente Vacas, 2002; Hyodo, Jido, and Hosaka, 2008; Garzon and Oset, 2015). Here the $N^*(1535)$ and $N^*(1650)$ are explained as a $K\Sigma$ state together with strong vector meson component (Garzon and Oset, 2015). These coupled-channel model calculations are performed with the η treated as a pure octet state. In Jefferson Laboratory measurements, the $N^*(1535)$ contribution to η electroproduction was observed to fall away more slowly with increasing large Q^2 (up to about 7 GeV²) than expected for a meson-baryon bound system (Armstrong *et al.*, 1999; Dalton *et al.*, 2009; Aznauryan and Burkert, 2012; Burkert, 2018). This suggests a significant three-quark contribution. On the other hand, the low Q^2 (below 1 GeV²) longitudinal transition amplitude suggests the need for meson cloud or other $4q\bar{q}$ contributions to the $N^*(1535)$ wave function.

The branching ratios for the $N^*(1535)$ to decay to η -nucleon and pion-nucleon final states are approximately equal, about 45%. This result was interpreted by Olbrich *et al.* (2018) as evidence for a possible gluon anomaly contribution to the decay. The strong η coupling has also been interpreted in quark models with configuration mixing

between the $N^*(1535)$ and $N^*(1650)$ (Saghai and Li, 2001; Chiang *et al.*, 2003).

VI. THE η AND η' IN NUCLEI

There is presently vigorous experimental and theoretical activity aimed at understanding the η and η' in medium and to search for evidence of possible η and η' bound states in nuclei. Medium modifications need to be understood self-consistently within the interplay of confinement, spontaneous chiral symmetry breaking, and axial U(1) dynamics. In the limit of chiral restoration the pion decay constant f_π should go to zero and perhaps with scalar confinement the pion constituent-quark and pion-nucleon coupling constants should vanish with dissolution of the pion wave function.

One finds a small pion mass shift of the order of a few MeV in nuclear matter (Kienle and Yamazaki, 2004). Experiments with deeply bound pionic atoms reveal a reduction in the value of the pion decay constant $f_\pi^{*2}/f_\pi^2 = 0.64 \pm 0.06$ at nuclear matter density (Suzuki *et al.*, 2004). Kaons are observed to experience an effective mass drop for the K^- to about 270 MeV at 2 times nuclear matter density in heavy-ion collisions (Schroter *et al.*, 1994; Barth *et al.*, 1997). These heavy-ion experiments also suggest the effective mass of antiprotons is reduced by about 100–150 MeV below their mass in free space (Schroter *et al.*, 1994). What should we expect for η and η' ? How does the gluonic part of their mass change in nuclei?

Meson masses in nuclei are determined from the meson-nucleus optical potential and the scalar induced contribution to the meson propagator evaluated at zero three-momentum, $\vec{k} = 0$, in the nuclear medium. Let $k = (E, \vec{k})$ and m denote the four-momentum and mass of the meson in free space. Then one solves

$$k^2 - m^2 = \text{Re}\Pi(E, \vec{k}, \rho) \quad (41)$$

for $\vec{k} = 0$, where Π is the in-medium s -wave meson self-energy and ρ is the nuclear density. Contributions to the in-medium mass come from the coupling to the scalar σ field in the nucleus in mean field approximation, nucleon-hole, and resonance-hole excitations in the medium. For $\vec{k} = 0$, $k^2 - m^2 \sim 2m(m^* - m)$, where m^* is the effective mass in the medium. The mass shift $m^* - m$ is the depth or real part of the meson-nucleus optical potential. The imaginary part of the potential measures the width of the meson in the nuclear medium. The s -wave self-energy can be written as (Ericson and Weise, 1988)

$$\Pi(E, \vec{k}, \rho)|_{\{\vec{k}=0\}} = -4\pi\rho \left(\frac{b}{1 + b\langle 1/r \rangle} \right). \quad (42)$$

Here $b = a(1 + m/M)$, where a is the meson-nucleon scattering length, M is the nucleon mass, and $\langle 1/r \rangle$ is the inverse correlation length, $\langle 1/r \rangle \simeq m_\pi$ for nuclear matter density. Attraction corresponds to positive values of a . The denominator in Eq. (42) is the Ericson-Ericson-Lorentz-Lorenz double scattering correction.

Studies involving bound state searches and excitation functions of mesons in photoproduction from nuclear targets give information about the meson-nucleus optical potential.

With a strong attractive interaction there is a chance to form meson bound states in nuclei (Haider and Liu, 1986). If found, these mesic nuclei would be a new state of matter bound just by the strong interaction. They differ from mesonic atoms (Yamazaki *et al.*, 1996) where, for example, a π^- is trapped in the Coulomb potential of the nucleus and bound by the electromagnetic interaction (Toki *et al.*, 1989).

Early experiments with low statistics using photon (Baskov *et al.*, 2012; Pheron *et al.*, 2012), pion (Chrien *et al.*, 1988), proton (Budzanowski *et al.*, 2009b), or deuteron (Moskal and Smyrski, 2010; Afanasiev *et al.*, 2011) beams gave hints for possible η mesic bound states but no clear signal (Kelkar *et al.*, 2013; Metag, Nanova, and Paryev, 2017). New COSY searches have focused on possible η bound states in ^3He and ^4He (Adlarson *et al.*, 2013, 2017b). η bound states in helium require a large η -nucleon scattering length with real part greater than about 0.7–1.1 fm (Barnea *et al.*, 2017; Barnea, Friedman, and Gal, 2017; Fix and Kolesnikov, 2017). At J-PARC the search for η -mesic nuclei is planned using pion induced reactions on ^7Li and ^{12}C targets (Fujioka, 2010). Recent measurements of η' photoproduction from nuclear targets have been interpreted to mean a small η' width in nuclei 20 ± 5.0 MeV at nuclear matter density ρ_0 (Nanova *et al.*, 2012) that might give rise to relatively narrow bound η' -nucleus states accessible to experiments. New experimental groups are looking for possible η' bound states in carbon using the (p, d) reaction at GSI/FAIR (Tanaka *et al.*, 2016, 2018), and photoproduction studies at Spring-8 with carbon and copper (Shimizu, 2017). Exciting possibilities could also be explored at ELSA in Bonn (Metag, 2015). For clean observation of a bound state one needs larger attraction than absorption and thus the real part of the meson-nucleus optical potential needs to be much bigger than the imaginary part.

A. The η' in medium

The η' -nucleus optical potential has been measured by the CBELSA/TAPS Collaboration in Bonn through studies of excitation functions in photoproduction experiments from nuclear targets. In photoproduction experiments the production cross section is enhanced with the lower effective meson mass in the nuclear medium. When the meson leaves the nucleus it returns on shell to its free mass with the energy budget conserved at the expense of the kinetic energy so that excitation functions and momentum distributions can provide essential clues to the meson properties in medium (Metag *et al.*, 2012; Weil, Mosel, and Metag, 2013).

Using this physics a first (indirect) estimate of the η' mass shift has recently been deduced by the CBELSA/TAPS Collaboration (Nanova *et al.*, 2013). The η' -nucleus optical potential $V_{\text{opt}} = V_{\text{real}} + iW$ deduced from these photoproduction experiments with a carbon target is

$$\begin{aligned} V_{\text{real}}(\rho_0) &= m^* - m = -37 \pm 10 \pm 10 \text{ MeV}, \\ W(\rho_0) &= -10 \pm 2.5 \text{ MeV} \end{aligned} \quad (43)$$

at nuclear matter density ρ_0 . In this experiment the average momentum of the produced η' was 1.1 GeV. The experiment was repeated with a niobium target with results $V_{\text{real}}(\rho_0) = -41 \pm 10 \pm 15$ MeV and $W(\rho_0) = -13 \pm 3 \pm 3$ MeV (Friedrich *et al.*, 2016; Nanova *et al.*, 2016). This optical potential corresponds to an effective scattering length in medium with real part about 0.5 fm in mean field approximation [switching off the Ericson-Ericson rescattering denominator in Eq. (42)], consistent with the COSY-11 and photoproduction values, Eqs. (38) and (39). These numbers with small width in medium suggest that bound states may be within reach of forthcoming experiments.

The transparency of nuclei to propagating mesons is illustrated through Fig. 6. Here the cross sections for meson production are parametrized by

$$\sigma(A) = \sigma_0 A^{\alpha(T)}, \quad (44)$$

where σ_0 is the photoproduction cross section from a free nucleon and α is a parameter depending on the meson and its kinetic energy. The value $\alpha \approx 1$ implies no absorption while $\alpha \approx 2/3$ corresponds to the meson being emitted only from the nuclear surface and thus strong absorption inside the nucleus. Figure 6 shows that the nucleus is approximately transparent to low-energy pions up to the threshold for Δ resonance excitation when α drops to around $2/3$, rising slightly at higher energies. The η and ω mesons have strong absorption. For η' one finds $\alpha \approx 0.84 \pm 0.03$ averaged over all kinetic energies signifying weaker interaction with the nucleus.

The mass shift, Eq. (43), is very similar to the expectations of the quark meson coupling (QMC) model (Bass and Thomas, 2006). In the QMC model medium modifications are calculated at the quark level through coupling of the light quarks in the hadron to the scalar isoscalar σ (and also ω and ρ) mean fields in the nucleus; for a review, see Guichon (1988), Guichon *et al.* (1996), and Saito, Tsushima, and Thomas (2007). One works in mean field approximation. The coupling constants for the coupling of light quarks to the σ (and ω and ρ) mean fields in the nucleus are adjusted to fit

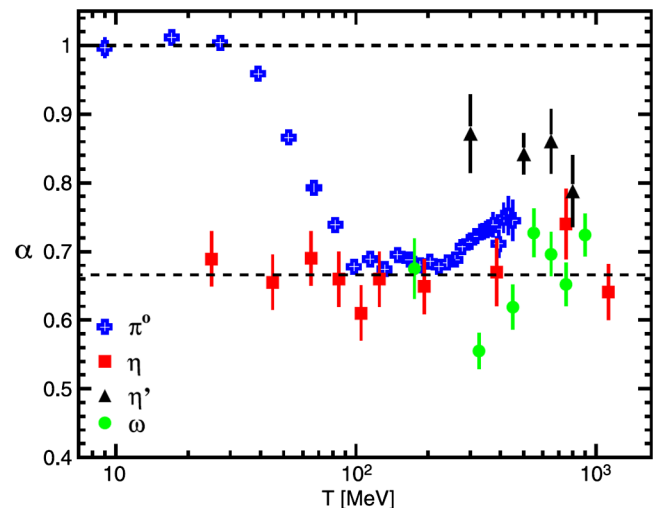


FIG. 6. Dependence of the parameter α [Eq. (44)] on the kinetic energy T of the mesons for π^0 , η , ω , and η' . From Nanova *et al.*, 2012.

the saturation energy and density of symmetric nuclear matter and the bulk symmetry energy. The large η and η' masses are used to motivate taking a Massachusetts Institute of Technology (MIT) bag description for the meson wave functions (Tsushima *et al.*, 1998; Tsushima, 2000). Phenomenologically, the MIT bag model gives a good fit to meson properties in free space for the kaons and heavier hadrons (DeGrand *et al.*, 1975). Gluonic topological effects are understood to be “frozen in,” meaning that they are only present implicitly through the masses and mixing angle in the model. The strange-quark component of the wave function does not couple to the σ mean field and η - η' mixing is readily built into the model. Possible binding energies and the in-medium masses of the η and η' are sensitive to the flavor-singlet component in the mesons and hence to the nonperturbative glue associated with axial U(1) dynamics (Bass and Thomas, 2006). Working with the mixing scheme in Eq. (13) with an η - η' mixing angle of -20° the QMC prediction for the η' mass in medium at nuclear matter density is 921 MeV; that is a mass shift of -37 MeV. This value is in excellent agreement with the mass shift $-37 \pm 10 \pm 10$ MeV deduced from photoproduction data, Eq. (43). Mixing increases the octet relative to the singlet component in η' , reducing the binding through increased a strange-quark component in the η' wave function. Without the gluonic mass contribution the η' would be a strange-quark state after η - η' mixing. Within the QMC model there would be no coupling to the σ mean field and no mass shift so that any observed mass shift is induced by glue associated with the QCD axial anomaly that generates part of the η' mass. For the η meson the potential depth predicted by QMC is ≈ -100 MeV at nuclear matter density with -20° mixing. For a pure octet η the model predicts a mass shift of ≈ -50 MeV. Increasing the flavor-singlet component in η at the expense of the octet component gives more attraction, more binding, and a larger value of the η -nucleon scattering length $a_{\eta N}$.

In QMC η - η' mixing with the phenomenological mixing angle -20° leads to a factor of 2 increase in the mass shift and in the scattering length obtained in the model relative to the prediction for a pure octet η_8 (Bass and Thomas, 2006). This result may explain why values of $a_{\eta N}$ extracted from phenomenological fits to experimental data where the η - η' mixing angle is unconstrained give larger values (with real part about 0.9 fm) than those predicted in theoretical coupled-channel models where η is treated as a pure octet state; see Sec. V.

Recent coupled-channel model calculations have appeared with mixing and vector meson channels included, with predictions for η' bound states for a range of possible values of $a_{\eta N}$ (Nagahiro *et al.*, 2012). Larger mass shifts, downward by up to 80–150 MeV, were found in Nambu–Jona-Lasinio (NJL) model calculations (without confinement) (Nagahiro, Takizawa, and Hirenzaki, 2006) and in linear sigma model calculations (in a hadronic basis) (Sakai and Jido, 2013) which also gave a rising η effective mass at finite density. Different QCD inspired models of the η and η' nucleus systems are constructed with different selections of “good physics input”: how they treat confinement, chiral symmetry, and axial U(1) dynamics. These different theoretical results raise interesting questions about the role of confinement and how massive light

pseudoscalar states can be for their wave functions to be treated as pure Goldstone bosons in the models.

Experiments in heavy-ion collisions (Averbeck *et al.*, 1997) and η photoproduction from nuclei (Roebig-Landau *et al.*, 1996; Yorita *et al.*, 2000) suggest little modification of the $N^*(1535)$ excitation in medium, although some evidence for the broadening of the $N^*(1535)$ in nuclei was reported by Yorita *et al.* (2000). In the QMC model the excitation energy is ~ 1544 MeV, consistent with observations, with the scalar attraction compensated by repulsion from coupling to the ω mean field (Bass and Thomas, 2006). The QMC model predictions for the kaon and proton mass shifts are a reduction in the K^- mass of about 100 MeV and effective proton mass about 755 MeV at nuclear matter density (Saito, Tsushima, and Thomas, 2007).

The first experiments to search for possible η' bound states in carbon have been performed at GSI with inclusive measurement of the $^{12}\text{C}(p, d)$ reaction (Tanaka *et al.*, 2016, 2018); see Fig. 7. These experiments exclude very deeply bound narrow states corresponding to real parts of the optical potential larger than about 150 MeV predicted (Nagahiro, Takizawa, and Hirenzaki, 2006; Nagahiro *et al.*, 2013) based on the NJL model when assuming the η' absorption (imaginary part of the potential of -10 MeV) deduced from measurements of the transparency in nuclei, Eq. (44) (Nanova *et al.*, 2012; Friedrich *et al.*, 2016). More precise studies are planned using semi-inclusive and exclusive measurements with the registration of the decay products of the mesic state (Tanaka *et al.*, 2017).

B. η mesic nuclei

Hints for possible η helium bound states are inferred from observed strong interaction in the η helium system. One finds a sharp rise in the cross section at threshold for η production both in photoproduction from ^3He and in the proton-deuteron reaction $dp \rightarrow ^3\text{He}\eta$, which may hint at a reduced η effective

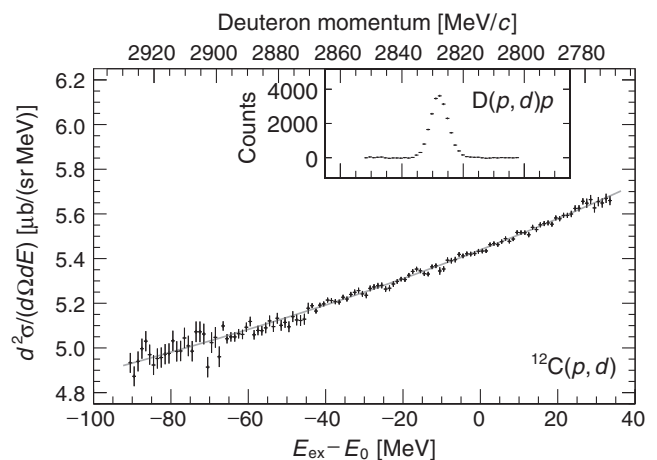


FIG. 7. Excitation spectrum of ^{11}C measured in the $^{12}\text{C}(p, d)$ reaction at a proton energy of 2.5 GeV. The horizontal axis is the excitation energy E_{ex} referring to the η' emission threshold $E_0 = 957.78$ MeV. The solid gray curve displays a fit with a third-order polynomial. The inset displays a momentum spectrum of the deuterons in the calibration $D(p, d)p$ reaction at 1.6 GeV. From Tanaka *et al.*, 2016, 2017.

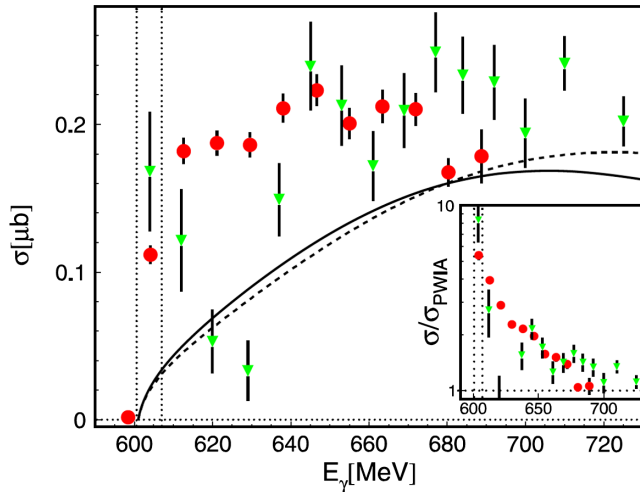


FIG. 8. Total cross section for the $\gamma^3\text{He} \rightarrow \eta^3\text{He}$ reaction. Data are from Pheron *et al.* (2012) (red points) and Pfeiffer *et al.* (2004) (green down triangles). Solid (dashed) curves represent plane wave impulse approximation (PWIA) calculations with a realistic (isotropic) angular distribution for the $\gamma n \rightarrow n\eta$ reaction. Inset: Ratio of measured and PWIA cross sections. From Pheron *et al.*, 2012.

mass in the nuclear medium. For these data, see Figs. 8 and 9, respectively. One also finds a small and constant value of the analyzing power (Papenbrock *et al.*, 2014) as well as strong variation of the angular asymmetry for η meson emission (Mersmann *et al.*, 2007; Smyrski *et al.*, 2007) indicating strong changes of the phase of the s -wave production amplitude with energy, as expected with a bound or virtual $^3\text{He} - \eta$ state (Wilkin *et al.*, 2007). A sharp but less steep rise in the cross section is also seen in the $dd \rightarrow ^4\text{He}\eta$ reaction (Frascaria *et al.*, 1994; Willis *et al.*, 1997; Wronska *et al.*, 2005; Budzanowski *et al.*, 2009a).

Searches for η mesic nuclei are ongoing with data from the WASA-at-COSY experiment. The focus has so far been on the

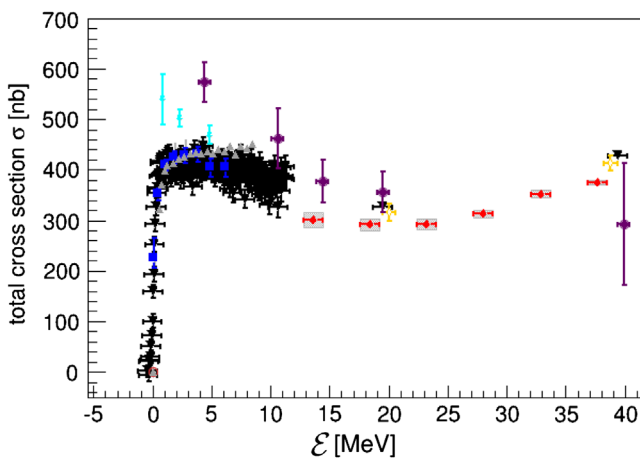


FIG. 9. World data on the $pd \rightarrow ^3\text{He}\eta$ reaction close to threshold (Berger *et al.*, 1988; Mayer *et al.*, 1996; Betigeri *et al.*, 2000; Bilger *et al.*, 2002; Adam *et al.*, 2007; Mersmann *et al.*, 2007; Smyrski *et al.*, 2007; Rausmann *et al.*, 2009; Adlarson *et al.*, 2014a, 2018c). Notice the sharp rise at threshold. Adapted from Adlarson *et al.*, 2018c.

reaction $dd \rightarrow ^3\text{He}N\pi$, in particular, studies of the excitation function around the threshold for $dd \rightarrow ^4\text{He}\eta$. These excitation functions did not reveal a structure that could be interpreted as a narrow mesic nucleus. Upper limits for the total cross sections for bound state production and decay in the processes $dd \rightarrow (^4\text{He} - \eta)_{\text{bound}} \rightarrow ^3\text{He}n\pi^0$ and $dd \rightarrow (^4\text{He} - \eta)_{\text{bound}} \rightarrow ^3\text{He}p\pi^-$ were determined assuming the mesic bound state width lies in the range 5–50 MeV. Taking into account recent results on the $N^*(1535)$ momentum distribution in the $N^*-^3\text{He}$ nucleus (Kelkar, 2016; Kelkar, Bedoya Fierro, and Moskal, 2016), the latest upper limits are about 5 and 10 nb for the $n\pi^0$ and $p\pi^-$ channels, respectively (Adlarson *et al.*, 2017b). These upper limits can be compared to model predictions. For example, within the optical model of Ikeno *et al.* (2017) most of the model parameter space is excluded allowing values of the real and imaginary parts of the potential only between zero and about -60 and -7 MeV, respectively (Skurzok *et al.*, 2018). While the achieved experimental sensitivity of a few nanobarns is too small to make definite conclusions about the existence of a $^4\text{He}-\eta$ bound state, the situation with ^3He may be more positive. The measurements have similar accuracy of the order of a few nanobarns with the expected bound state production cross sections for $pd \rightarrow (^3\text{He}-\eta)_{\text{bound}}$ (Wilkin, 2014) expected to be more than 20 times larger than for $dd \rightarrow (^4\text{He}-\eta)_{\text{bound}}$ (Wycech and Krzemiński, 2014). Data analysis for the pd reaction is ongoing (Rundel *et al.*, 2017). Recent calculations in the framework of optical potential (Xie *et al.*, 2017), multibody calculations (Barnea, Friedman, and Gal, 2017), and pionless effective field theory (Barnea *et al.*, 2017) suggest a possible $^3\text{He}-\eta$ bound state.

C. The η' at finite temperature

In addition to finite density, axial U(1) symmetry is also expected to be partially restored at finite temperature (Kapusta, Kharzeev, and McLerran, 1996). This result is observed in recent QCD lattice calculations (Bazavov *et al.*, 2012; Cossu *et al.*, 2013; Tomiya *et al.*, 2017). Experimentally, there are hints in RHIC data from relativistic heavy-ion collisions for a possible η' mass suppression at finite temperature, with claims of at least -200 MeV mass shift deduced from studies of the intercept λ measured in two-charged-pion Bose-Einstein correlations (Csorgo, Vertesi, and Sziklai, 2010; Vertesi, Csorgo, and Sziklai, 2011). With decreasing η' mass one expects a drop in this parameter at small transverse momentum (Vance, Csorgo, and Kharzeev, 1998). The λ parameter accounts for the fact that not all pion pairs are correlated, e.g., as daughters of long-lived strongly decaying resonances and effects from the source dynamics. A key issue in the analysis here is the matching of this dilution factor between experiment and theory. The ALICE Collaboration at CERN see similar effects in the data to the RHIC experiments with λ falling by $\sim 70\%$ at the smallest transverse momentum without attempting an η' mass-shift extraction (Adam *et al.*, 2016).

VII. HIGH-ENERGY η AND η' PRODUCTION

In higher energy experiments with proton-proton collisions at 450 GeV, or center-of-mass energy of 28 GeV, the WA102

Collaboration at CERN observed that central production of η and η' mesons seems to have a similar production mechanism which differs from that of π^0 (Barberis *et al.*, 1998). This result has been interpreted in terms of gluonic pomeron-pomeron and pomeron-Reggeon fusion (Close and Schuler, 1999; Lebedowicz, Nachtmann, and Szczurek, 2014). The pomeron is a nonperturbative color-singlet combination of gluon exchange which governs the high-energy behavior of hadron scattering processes. Reggeons involve the sum over mesonlike exchanges carrying particular quantum numbers in these reactions (Collins and Martin, 1984; Landshoff, 1994).

Semi-inclusive η production in high-energy collisions has been a topical issue since the pioneering work of Field and Feynman (1977). One finds the interesting result that the ratio of η to π^0 production rises rapidly with the transverse momentum p_t of the produced meson and levels off at $R_{\eta/\pi^0} \sim 0.4\text{--}0.5$ above $p_t \sim 2$ GeV in nuclear collisions (proton-proton, proton-nucleus, and nucleus-nucleus) independent of the colliding nuclei; see Fig. 10. These results hold over a wide range of center-of-mass energy ($\sqrt{s_{NN}} \sim 30\text{--}8000$ GeV) as well as meson production carrying momentum fraction $x_p > 0.35$ of the exchanged photon in electron-positron collisions at LEP, $\sqrt{s} = 91.2$ GeV.

In these relativistic heavy-ion collisions the invariant yields per nucleon-nucleon collision are increasingly depleted with centrality in comparison to proton-proton results at the same center-of-mass energy. The maximum suppression factor is about 5 in central Au + Au collisions (Adler *et al.*, 2006). The measured η/π^0 ratio is independent of both the reaction centrality as well as the species of colliding protons or nuclei. These results indicate that any initial and/or final state nuclear effects influence the production of light neutral mesons at large p_t in the same way. The approximately constant ratio for η to π^0 production indicates that the parent quark or gluon parton first loses energy in the dense medium of the collision and then fragments into leading mesons η and π^0 in the vacuum according to the same probabilities that govern high p_t hadron production in more elementary e^+e^- and proton-proton collisions. These results observed at RHIC in PHENIX

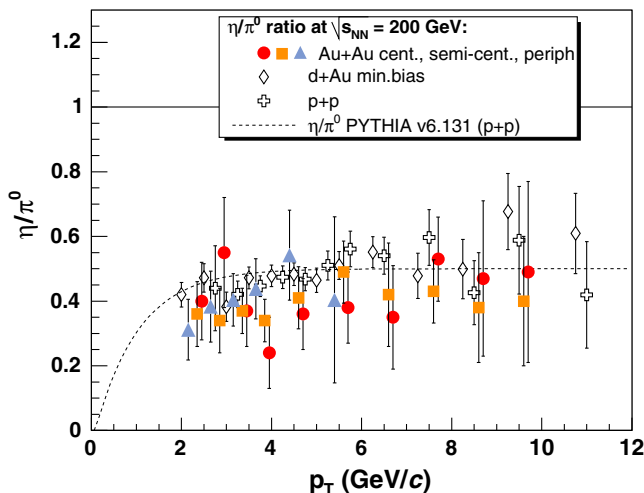


FIG. 10. Ratio of η to π^0 production in RHIC PHENIX data. From Adler *et al.*, 2006.

(Adler *et al.*, 2006, 2007) and STAR (Abelev *et al.*, 2010) data at $\sqrt{s_{NN}} = 200$ GeV are also observed by ALICE at the LHC up to 8 TeV (Acharya *et al.*, 2018a, 2018b, 2018c), with earlier measurements summarized by Adler *et al.* (2007).

The fragmentation functions for η production in high-energy processes were discussed by Aidala *et al.* (2011). First measurements of η' production in proton-proton collisions at center-of-mass energy 200 GeV are reported by the PHENIX Collaboration in Adare *et al.* (2011b). In ALEPH data from LEP η' production was observed to be anomalously suppressed compared to the expectations of string fragmentation models without an additional “ η' suppression factor,” possibly associated with the mass of the produced η' (Barate *et al.*, 2000). The cross section and double helicity asymmetry for η production was studied by PHENIX at midrapidity with comparison to π^0 production in Adare *et al.* (2011a). The transverse single-spin asymmetry for forward η production looks as large as if not larger than that for forward π^0 production—see PHENIX (Adare *et al.*, 2014) and STAR (Adamczyk *et al.*, 2012)—and may be related to quark-gluon correlation functions.

A. η' - π interactions and 1^{-+} exotics

Following the discussion in Sec. II, the OZI-violating interaction $\xi Q^2 \partial_\mu \pi_a \partial^\mu \pi_a$ gives a potentially important tree-level contribution to the decay $\eta' \rightarrow \eta \pi \pi$ (Di Vecchia *et al.*, 1981). Suppose one takes ξ as negative with attractive interaction. When iterated in the Bethe-Salpeter equation for $\eta' \pi$ rescattering this interaction then yields a dynamically generated resonance with quantum numbers $J^{PC} = 1^{-+}$ and mass about 1400 MeV. The dynamics here is mediated by the singlet OZI-violating coupling of η' (Bass and Marco, 2002). One finds a possible dynamical interpretation of light-mass 1^{-+} exotic states, e.g., as observed in experiments at BNL (Thompson *et al.*, 1997; Adams *et al.*, 1998; Chung *et al.*, 1999; Ivanov *et al.*, 2001) and CERN (Abele *et al.*, 1998); see also Szczepaniak *et al.* (2003). This OZI-violating interaction will also contribute to higher L odd partial waves with quantum numbers L^{-+} . These states are particularly interesting because the quantum numbers $1^{-+}, 3^{-+}, 5^{-+}, \dots$ are inconsistent with a simple quark-antiquark bound state. The COMPASS experiment at CERN has recently measured exclusive production of $\eta' \pi^-$ and $\eta \pi^-$ in 191 GeV π^- collisions on a hydrogen target (Adolph *et al.*, 2015). They found the interesting result that $\eta' \pi^-$ production is enhanced relative to $\eta \pi^-$ production by a factor of 5–10 in the exotic $L = 1, 3, 5$ partial waves with quantum numbers L^{-+} in the inspected invariant mass range up to 3 GeV; see Fig. 11. No enhancement was observed in the even L partial waves. For further recent discussion, see also Rodas *et al.* (2018).

Glueballs, postulated bound states of gluons with integer spin, may also couple strongly to η' and η . Glueball states are found in lattice pure glue theory with mixing with quark-antiquark mesons induced in full QCD (Morningstar and Peardon, 1999; E. Gregory *et al.*, 2012; Gui *et al.*, 2013; Sun *et al.*, 2017). The lightest glueball state is expected to be a scalar with the prime candidates discussed in the literature being the $f_0(1500)$ and $f_0(1710)$ states, much heavier than the lightest mass quark-antiquark state—the pseudoscalar pion. We refer to Frere and Heeck (2015) and Brunner and

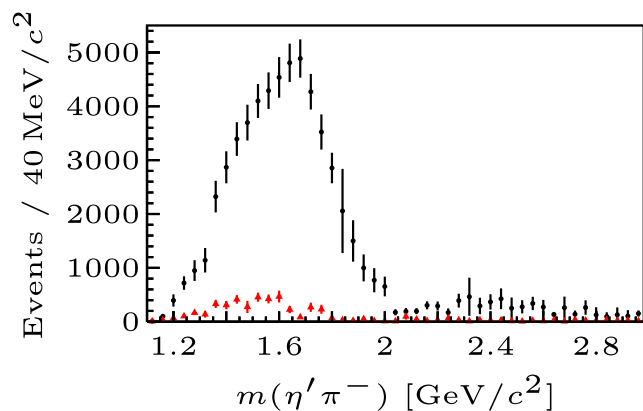


FIG. 11. The $\eta'\pi^-$ exotic partial wave 1^{-+} (upper data) is much enhanced compared to $\eta\pi^-$ (lower data) in exclusive production from 191 GeV π^- scattering on a hydrogen fixed target. From Adolph *et al.*, 2015.

Rebhan (2015) for recent discussions of scalar glueball decays to η and η' final states. Particularly interesting is a pseudoscalar glueball in the mass range 2–3 GeV where recent calculations suggest a narrow state and very restricted decay pattern involving η or η' mesons that can be searched for in central exclusive production experiments, e.g., at the LHC (Brunner and Rebhan, 2017).

VIII. SUMMARY AND FUTURE CHALLENGES

The isoscalar η and η' mesons are sensitive to the interface of chiral and nonperturbative dynamics. One finds a rich phenomenology involving OZI violation, meson production dynamics from threshold through to high-energy collisions, and the coupling to new excited nucleon resonances. Axial U(1) symmetry is expected to be partially restored in QCD media at finite densities and temperature. This, in turn, leads to predictions for the η and η' effective mass shifts in medium and possible meson bound states in nuclei. The nonperturbative glue which generates the large η and η' masses also has the potential to induce strong CP violation in the neutron electric dipole moment which is not observed. A possible solution to this strong CP puzzle is connected with a new axion particle which, if it exists, might also be associated with dark matter. Understanding the η and η' systems is important to nuclear, high energy, and astrophysics.

New experiments will give valuable insight into η and η' physics. The search for η and η' mesic nuclei will help pin down the dynamics of axial U(1) symmetry breaking in low-energy QCD. Determining the η' properties at finite temperature in relativistic heavy-ion collisions would further probe axial U(1) dynamics in the QCD phase diagram. Precision studies of η and η' decays are a probe for new physics beyond the standard model. Production of η' mesons in connection with glueball production will test theoretical ideas about gluonic excitations in nonperturbative QCD.

ACKNOWLEDGMENTS

We thank C. Aidala, V. Burkert, M. Faessler, A. Fix, S. Hirenzaki, K. Itahashi, J. Krzysiak, W. Melnitchouk,

V. Metag, G. Moskal, E. Oset, M. Pitschmann, A. Rebhan, H. Shimizu, M. Silarski, M. Skurzok, Y. Tanaka, A. W. Thomas, and M. Weber for helpful discussions. We acknowledge support from the Polish National Science Centre through Grant No. 2016/23/B/ST2/00784 and the Foundation for Polish Science through the TEAM/2017-4/39 programme.

REFERENCES

- Abdel-Bary, M., *et al.* (TOF Collaboration), 2003, *Eur. Phys. J. A* **16**, 127.
- Abel, C., *et al.*, 2017, *Phys. Rev. X* **7**, 041034.
- Abele, A., *et al.* (Crystal Barrel Collaboration), 1998, *Phys. Lett. B* **423**, 175.
- Abelev, B. I., *et al.* (STAR Collaboration), 2010, *Phys. Rev. C* **81**, 064904.
- Ablikim, M., *et al.* (BESIII Collaboration), 2015a, *Phys. Rev. D* **92**, 012014.
- Ablikim, M., *et al.* (BESIII Collaboration), 2015b, *Phys. Rev. D* **92**, 012001.
- Ablikim, M., *et al.* (BESIII Collaboration), 2017, *Phys. Rev. Lett.* **118**, 012001.
- Accardi, A., *et al.*, 2016, *Eur. Phys. J. A* **52**, 268.
- Acharya, S., *et al.* (ALICE Collaboration), 2018a, *Phys. Rev. C* **98**, 044901.
- Acharya, S., *et al.* (ALICE Collaboration), 2018b, *Eur. Phys. J. C* **78**, 624.
- Acharya, S., *et al.* (ALICE Collaboration), 2018c, *Eur. Phys. J. C* **78**, 263.
- Adachi, I., *et al.* (Belle Collaboration), 2008, *Phys. Lett. B* **662**, 323.
- Adam, H. H., *et al.* (COSY-11 Collaboration), 2007, *Phys. Rev. C* **75**, 014004.
- Adam, J., *et al.* (ALICE Collaboration), 2016, *Phys. Rev. C* **93**, 024905.
- Adamczyk, L., *et al.* (STAR Collaboration), 2012, *Phys. Rev. D* **86**, 051101.
- Adams, G. S., *et al.* (E852 Collaboration), 1998, *Phys. Rev. Lett.* **81**, 5760.
- Adare, A., *et al.* (PHENIX Collaboration), 2011a, *Phys. Rev. D* **83**, 032001.
- Adare, A., *et al.* (PHENIX Collaboration), 2011b, *Phys. Rev. D* **83**, 052004.
- Adare, A., *et al.* (PHENIX Collaboration), 2014, *Phys. Rev. D* **90**, 072008.
- Adlarson, P., *et al.* (A2 Collaboration), 2017a, *Phys. Rev. C* **95**, 035208.
- Adlarson, P., *et al.* (WASA-at-COSY Collaboration), 2012, *Phys. Lett. B* **707**, 243.
- Adlarson, P., *et al.* (WASA-at-COSY Collaboration), 2013, *Phys. Rev. C* **87**, 035204.
- Adlarson, P., *et al.* (WASA-at-COSY Collaboration), 2014a, *Eur. Phys. J. A* **50**, 100.
- Adlarson, P., *et al.* (WASA-at-COSY Collaboration), 2014b, *Phys. Rev. C* **90**, 045207.
- Adlarson, P., *et al.* (WASA-at-COSY Collaboration), 2016, *Phys. Rev. C* **94**, 065206.
- Adlarson, P., *et al.* (WASA-at-COSY Collaboration), 2017b, *Nucl. Phys. A* **959**, 102.
- Adlarson, P., *et al.* (WASA-at-COSY Collaboration), 2018a, *arXiv:1802.08642*.
- Adlarson, P., *et al.* (WASA-at-COSY Collaboration), 2018b, *Phys. Rev. Lett.* **120**, 022002.

- Adlarson, P., *et al.* (WASA-at-COSY Collaboration), 2018c, *Phys. Lett. B* **782**, 297.
- Adler, S. L., 1969, *Phys. Rev.* **177**, 2426.
- Adler, S. S., *et al.* (PHENIX Collaboration), 2006, *Phys. Rev. Lett.* **96**, 202301.
- Adler, S. S., *et al.* (PHENIX Collaboration), 2007, *Phys. Rev. C* **75**, 024909.
- Adolph, C., *et al.* (COMPASS Collaboration), 2015, *Phys. Lett. B* **740**, 303.
- Adolph, C., *et al.* (WASA-at-COSY Collaboration), 2009, *Phys. Lett. B* **677**, 24.
- Afanasyev, S. V., *et al.*, 2011, *Phys. Part. Nucl. Lett.* **8**, 1073.
- Aidala, C. A., S. D. Bass, D. Hasch, and G. K. Mallot, 2013, *Rev. Mod. Phys.* **85**, 655.
- Aidala, C. A., F. Ellinghaus, R. Sassot, J. P. Seele, and M. Stratmann, 2011, *Phys. Rev. D* **83**, 034002.
- Al Ghol, H., *et al.* (GlueX Collaboration), 2017, *Phys. Rev. C* **95**, 042201.
- Altarelli, G., 2013, [arXiv:1303.2842](https://arxiv.org/abs/1303.2842).
- Ambrosino, F., *et al.* (KLOE Collaboration), 2007, *Phys. Lett. B* **648**, 267.
- Ambrosino, F., *et al.* (KLOE Collaboration), 2009, *J. High Energy Phys.* **07**, 105.
- Ambrosino, F., *et al.* (KLOE-2 Collaboration), 2010, *Phys. Lett. B* **694**, 16.
- Anastasi, A., *et al.* (KLOE-2 Collaboration), 2016, *J. High Energy Phys.* **05**, 019.
- Anisovich, A. V., V. Burkert, P. M. Collins, M. Dugger, E. Klempt, V. A. Nikonov, B. G. Ritchie, A. V. Sarantsev, and U. Thoma, 2017, *Phys. Lett. B* **772**, 247.
- Anisovich, A. V., V. Burkert, M. Dugger, E. Klempt, V. A. Nikonov, B. G. Ritchie, A. V. Sarantsev, and U. Thoma, 2018, *Phys. Lett. B* **785**, 626.
- Anisovich, A. V., E. Klempt, B. Krusche, V. A. Nikonov, A. V. Sarantsev, U. Thoma, and D. Werthmueller, 2015, *Eur. Phys. J. A* **51**, 72.
- Aoki, S., *et al.*, 2017, *Eur. Phys. J. C* **77**, 112.
- Armstrong, C. S., *et al.* (Jefferson Lab E94014 Collaboration), 1999, *Phys. Rev. D* **60**, 052004.
- Arnaldi, R., *et al.* (NA60 Collaboration), 2009, *Phys. Lett. B* **677**, 260.
- Arndt, R. A., W. J. Briscoe, T. W. Morrison, I. I. Strakovsky, R. L. Workman, and A. B. Gridnev, 2005, *Phys. Rev. C* **72**, 045202.
- Atwood, D., and A. Soni, 1997, *Phys. Lett. B* **405**, 150.
- Aubert, B., *et al.* (BABAR Collaboration), 2001, [arXiv:hep-ex/0109034](https://arxiv.org/abs/hep-ex/0109034).
- Averbeck, R., *et al.* (TAPS Collaboration), 1997, *Z. Phys. A* **359**, 65.
- Aznauryan, I. G., and V. D. Burkert, 2012, *Prog. Part. Nucl. Phys.* **67**, 1.
- Babusci, D., *et al.* (KLOE-2 Collaboration), 2013a, *J. High Energy Phys.* **01**, 119.
- Babusci, D., *et al.* (KLOE-2 Collaboration), 2013b, *Phys. Lett. B* **718**, 910.
- Balestra, F., *et al.* (DISTO Collaboration), 2000, *Phys. Lett. B* **491**, 29.
- Bali, G., S. Collins, and J. Simeth, 2018, *EPJ Web Conf.* **175**, 05028.
- Bali, G. S., S. Collins, S. Drr, and I. Kanamori, 2015, *Phys. Rev. D* **91**, 014503.
- Ball, P., J. M. Frere, and M. Tytgat, 1996, *Phys. Lett. B* **365**, 367.
- Barate, R., *et al.* (ALEPH Collaboration), 2000, *Eur. Phys. J. C* **16**, 613.
- Barberis, D., *et al.* (WA102 Collaboration), 1998, *Phys. Lett. B* **427**, 398.
- Barnea, N., B. Bazak, E. Friedman, and A. Gal, 2017, *Phys. Lett. B* **771**, 297; **775**, 364(E) (2017).
- Barnea, N., E. Friedman, and A. Gal, 2017, *Nucl. Phys. A* **968**, 35.
- Barth, R., *et al.* (KaoS Collaboration), 1997, *Phys. Rev. Lett.* **78**, 4007.
- Baskov, V. A., *et al.*, 2012, *Proc. Sci. Baldin-ISHEPP-XXI*, 102.
- Bass, S. D., 1999, *Phys. Lett. B* **463**, 286.
- Bass, S. D., 2000, [arXiv:hep-ph/0006348](https://arxiv.org/abs/hep-ph/0006348).
- Bass, S. D., 2005, *Rev. Mod. Phys.* **77**, 1257.
- Bass, S. D., 2009, *Acta Phys. Pol. B Proc. Suppl.* **2**, 11 [<http://www.actaphys.uj.edu.pl/fulltext?series=Sup&vol=2&page=11>].
- Bass, S. D., and E. Marco, 2002, *Phys. Rev. D* **65**, 057503.
- Bass, S. D., and A. W. Thomas, 2006, *Phys. Lett. B* **634**, 368.
- Bass, S. D., and A. W. Thomas, 2010, *Phys. Lett. B* **684**, 216.
- Bass, S. D., and A. W. Thomas, 2014, *Acta Phys. Pol. B* **45**, 627.
- Baudis, L., 2018, [arXiv:1801.08128](https://arxiv.org/abs/1801.08128).
- Baur, R., J. Kambor, and D. Wyler, 1996, *Nucl. Phys. B* **460**, 127.
- Bazavov, A., *et al.* (HotQCD Collaboration), 2012, *Phys. Rev. D* **86**, 094503.
- Behrend, H. J., *et al.* (CELLO Collaboration), 1991, *Z. Phys. C* **49**, 401.
- Behrens, B. H., *et al.* (CLEO Collaboration), 1998, *Phys. Rev. Lett.* **80**, 3710.
- Bell, J. S., and R. Jackiw, 1969, *Nuovo Cimento A* **60**, 47.
- Bennett, G. W., *et al.* (Muon g-2 Collaboration), 2006, *Phys. Rev. D* **73**, 072003.
- Bergdolt, A. M., *et al.*, 1993, *Phys. Rev. D* **48**, R2969.
- Berger, J., *et al.* (SPES4 Collaboration), 1988, *Phys. Rev. Lett.* **61**, 919.
- Betigeri, M., *et al.* (GEM Collaboration), 2000, *Phys. Lett. B* **472**, 267.
- Bijnens, J., G. Faldt, and B. M. K. Nefkens, 2002, Eds., *Proceedings, Workshop, Uppsala, Sweden, 2001* [*Phys. Scr.* **T99**, 1] [<http://inspirehep.net/record/599222>].
- Bilger, R., *et al.* (WASA/PROMICE Collaboration), 2002, *Phys. Rev. C* **65**, 044608.
- Braun-Munzinger, P., and J. Wambach, 2009, *Rev. Mod. Phys.* **81**, 1031.
- Browder, T. E., *et al.* (CLEO Collaboration), 1998, *Phys. Rev. Lett.* **81**, 1786.
- Brunner, F., and A. Rebhan, 2015, *Phys. Rev. D* **92**, 121902.
- Brunner, F., and A. Rebhan, 2017, *Phys. Lett. B* **770**, 124.
- Budzanowski, A., *et al.* (GEM Collaboration), 2009a, *Nucl. Phys. A* **821**, 193.
- Budzanowski, A., *et al.* (GEM Collaboration), 2009b, *Phys. Rev. C* **79**, 012201.
- Burkert, V. D., 2018, *Few-Body Syst.* **59**, 57.
- Calen, H., *et al.* (WASA/PROMICE Collaboration), 1996, *Phys. Lett. B* **366**, 39.
- Calen, H., *et al.* (WASA/PROMICE Collaboration), 1998, *Phys. Rev. C* **58**, 2667.
- Chiang, W.-T., S. N. Yang, M. Vanderhaeghen, and D. Drechsel, 2003, *Nucl. Phys. A* **723**, 205.
- Chiavassa, E., *et al.* (PINOT Collaboration), 1994, *Phys. Lett. B* **322**, 270.
- Chrien, R. E., *et al.*, 1988, *Phys. Rev. Lett.* **60**, 2595.
- Christ, N. H., C. Dawson, T. Izubuchi, C. Jung, Q. Liu, R. D. Mawhinney, C. T. Sachrajda, A. Soni, and R. Zhou, 2010, *Phys. Rev. Lett.* **105**, 241601.
- Chung, S. U., *et al.* (E852 Collaboration), 1999, *Phys. Rev. D* **60**, 092001.
- Cichy, K., E. Garcia-Ramos, K. Jansen, K. Otnad, and C. Urbach (ETM), 2015, *J. High Energy Phys.* **09**, 020.

- Close, F.E., 1979, *An Introduction to Quarks and Partons* (Academic Press, London).
- Close, F.E., and G. A. Schuler, 1999, *Phys. Lett. B* **464**, 279.
- Colangelo, G., S. Lanz, H. Leutwyler, and E. Passemar, 2017, *Phys. Rev. Lett.* **118**, 022001.
- Collins, P., *et al.*, 2017, *Phys. Lett. B* **771**, 213.
- Collins, P. D. B., and A. D. Martin, 1984, *Hadron Interactions* (Adam Hilger, Bristol, UK).
- Cossu, G., S. Aoki, H. Fukaya, S. Hashimoto, T. Kaneko, H. Matsufuru, and J.-I. Noaki, 2013, *Phys. Rev. D* **87**, 114514; **88**, 019901(E) (2013).
- Crede, V., *et al.* (CBELSA/TAPS Collaboration), 2009, *Phys. Rev. C* **80**, 055202.
- Crewther, R. J., 1978, *Acta Phys. Austriaca Suppl.* **19**, 47.
- Crewther, R. J., P. Di Vecchia, G. Veneziano, and E. Witten, 1979, *Phys. Lett. B* **88**, 123; **91**, 487(E) (1980).
- Csorgo, T., R. Vertesi, and J. Sziklai, 2010, *Phys. Rev. Lett.* **105**, 182301.
- Czerwinski, E., P. Moskal, and M. Silarski (COSY-11 Collaboration), 2014, *Acta Phys. Pol. B* **45**, 739.
- Czerwinski, E., *et al.* (COSY-11 Collaboration), 2010, *Phys. Rev. Lett.* **105**, 122001.
- Czerwinski, E., *et al.* (COSY-11 Collaboration), 2014, *Phys. Rev. Lett.* **113**, 062004.
- Czyzykiewicz, R., *et al.* (COSY-11 Collaboration), 2007, *Phys. Rev. Lett.* **98**, 122003.
- Dalton, M. M., *et al.*, 2009, *Phys. Rev. C* **80**, 015205.
- Dashen, R. F., 1969, *Phys. Rev.* **183**, 1245.
- DeGrand, T. A., R. L. Jaffe, K. Johnson, and J. E. Kiskis, 1975, *Phys. Rev. D* **12**, 2060.
- del Amo Sanchez, P., *et al.* (BABAR Collaboration), 2011, *Phys. Rev. D* **84**, 052001.
- Deloff, A., 2004, *Phys. Rev. C* **69**, 035206.
- Deshpande, A., 2017, *Int. J. Mod. Phys. E* **26**, 1740007.
- Di Donato, C., G. Ricciardi, and I. Bigi, 2012, *Phys. Rev. D* **85**, 013016.
- Dighe, A. S., M. Gronau, and J. L. Rosner, 1996, *Phys. Lett. B* **367**, 357; **377**, 325(E) (1996).
- Dighe, A. S., M. Gronau, and J. L. Rosner, 1997, *Phys. Rev. Lett.* **79**, 4333.
- Di Vecchia, P., F. Nicodemi, R. Pettorino, and G. Veneziano, 1981, *Nucl. Phys. B* **181**, 318.
- Di Vecchia, P., and G. Veneziano, 1980, *Nucl. Phys. B* **171**, 253.
- Dugger, M., *et al.* (CLAS Collaboration), 2006, *Phys. Rev. Lett.* **96**, 062001; **96**, 169905(E) (2006).
- Ellis, J., 2014, *Int. J. Mod. Phys. A* **29**, 1430072.
- Ericson, T. E. O., and W. Weise, 1988, *Pions and Nuclei* (Clarendon Press, Oxford, UK).
- Escribano, R., and J.-M. Frere, 2005, *J. High Energy Phys.* **06**, 029.
- Escribano, R., and J. Nadal, 2007, *J. High Energy Phys.* **05**, 006.
- Fäldt, G., and C. Wilkin, 1996, *Phys. Lett. B* **382**, 209.
- Fäldt, G., and C. Wilkin, 2001, *Phys. Scr.* **64**, 427.
- Fang, S.-s., A. Kupsc, and D.-h. Wei, 2018, *Chin. Phys. C* **42**, 042002.
- Feldmann, T., 2000, *Int. J. Mod. Phys. A* **15**, 159.
- Feldmann, T., and P. Kroll, 1998, *Eur. Phys. J. C* **5**, 327.
- Feldmann, T., P. Kroll, and B. Stech, 1998, *Phys. Rev. D* **58**, 114006.
- Field, R. D., and R. P. Feynman, 1977, *Phys. Rev. D* **15**, 2590.
- Fix, A., and O. Kolesnikov, 2017, *Phys. Lett. B* **772**, 663.
- Frascaria, R., *et al.* (SPES4 Collaboration), 1994, *Phys. Rev. C* **50**, R537.
- Frere, J.-M., and J. Heeck, 2015, *Phys. Rev. D* **92**, 114035.
- Friedrich, S., *et al.* (CBELSA/TAPS Collaboration), 2016, *Eur. Phys. J. A* **52**, 297.
- Fritzsch, H., 1997, *Phys. Lett. B* **415**, 83.
- Fritzsch, H., and P. Minkowski, 1975, *Nuovo Cimento A* **30**, 393.
- Fujioka, H., 2010, *Acta Phys. Pol. B* **41**, 2261.
- Garcia-Recio, C., J. Nieves, T. Inoue, and E. Oset, 2002, *Phys. Lett. B* **550**, 47.
- Garzon, E. J., and E. Oset, 2015, *Phys. Rev. C* **91**, 025201.
- Gasser, J., and H. Leutwyler, 1982, *Phys. Rep.* **87**, 77.
- Gauzzi, P. (KLOE-2 Collaboration), 2012, *J. Phys. Conf. Ser.* **349**, 012002.
- Gell-Mann, M., 1961, Caltech Report No. CTSL-20.
- Gell-Mann, M., R. J. Oakes, and B. Renner, 1968, *Phys. Rev.* **175**, 2195.
- Gell-Mann, M., and K. M. Watson, 1954, *Annu. Rev. Nucl. Part. Sci.* **4**, 219.
- Georgi, H., 1984, *Weak Interactions and Modern Particle Theory* (Benjamin/Cummings, Menlo Park).
- Gilman, F. J., and R. Kauffman, 1987, *Phys. Rev. D* **36**, 2761; **37**, 3348(E) (1988).
- Green, A. M., and S. Wycech, 1999, *Phys. Rev. C* **60**, 035208.
- Green, A. M., and S. Wycech, 2005, *Phys. Rev. C* **71**, 014001; **72**, 029902(E) (2005).
- Greensite, J., 2011, *Lect. Notes Phys.* **821**, 1.
- Gregory, E., A. Irving, B. Lucini, C. McNeile, A. Rago, C. Richards, and E. Rinaldi, 2012, *J. High Energy Phys.* **10**, 170.
- Gregory, E. B., A. C. Irving, C. M. Richards, and C. McNeile (UKQCD Collaboration), 2012, *Phys. Rev. D* **86**, 014504.
- Gronberg, J., *et al.* (CLEO Collaboration), 1998, *Phys. Rev. D* **57**, 33.
- Gui, L.-C., Y. Chen, G. Li, C. Liu, Y.-B. Liu, J.-P. Ma, Y.-B. Yang, and J.-B. Zhang (CLQCD Collaboration), 2013, *Phys. Rev. Lett.* **110**, 021601.
- Guichon, P. A. M., 1988, *Phys. Lett. B* **200**, 235.
- Guichon, P. A. M., K. Saito, E. N. Rodionov, and A. W. Thomas, 1996, *Nucl. Phys. A* **601**, 349.
- Guo, P., I. V. Danilkin, C. Fernández-Ramírez, V. Mathieu, and A. P. Szczepaniak, 2017, *Phys. Lett. B* **771**, 497.
- Gyulassy, M., and L. McLerran, 2005, *Nucl. Phys. A* **750**, 30.
- Haider, Q., and L. C. Liu, 1986, *Phys. Lett. B* **172**, 257.
- Hall, J. M. M., W. Kamleh, D. B. Leinweber, B. J. Menadue, B. J. Owen, A. W. Thomas, and R. D. Young, 2015, *Phys. Rev. Lett.* **114**, 132002.
- Harland-Lang, L. A., V. A. Khoze, M. G. Ryskin, and W. J. Stirling, 2013, *Eur. Phys. J. C* **73**, 2429.
- Hertzog, D. W., 2016, *EPJ Web Conf.* **118**, 01015.
- Hibou, F., *et al.* (SPES3 Collaboration), 1998, *Phys. Lett. B* **438**, 41.
- Hou, W.-S., and B. Tseng, 1998, *Phys. Rev. Lett.* **80**, 434.
- Hyodo, T., D. Jido, and A. Hosaka, 2008, *Phys. Rev. C* **78**, 025203.
- Iizuka, J., 1966, *Prog. Theor. Phys. Suppl.* **37**, 21.
- Ikeno, N., H. Nagahiro, D. Jido, and S. Hirenzaki, 2017, *Eur. Phys. J. A* **53**, 194.
- Inoue, T., and E. Oset, 2002, *Nucl. Phys. A* **710**, 354.
- Inoue, T., E. Oset, and M. J. Vicente Vacas, 2002, *Phys. Rev. C* **65**, 035204.
- Ioffe, B. L., 2006, *Int. J. Mod. Phys. A* **21**, 6249.
- Isgur, N., and G. Karl, 1978, *Phys. Rev. D* **18**, 4187.
- Ivanov, E. I., *et al.* (E852 Collaboration), 2001, *Phys. Rev. Lett.* **86**, 3977.
- Jaegle, I., *et al.* (CBELSA/TAPS Collaboration), 2011, *Eur. Phys. J. A* **47**, 11.
- Jarlskog, C., and E. Shabalin, 2002, *Phys. Scr.* **T99**, 23.
- Jegerlehner, F., 2017, *The Anomalous Magnetic Moment of the Muon*, Springer Tracts in Modern Physics, Vol. 274, pp. 1–693.

- Kaiser, N., P. B. Siegel, and W. Weise, 1995, *Phys. Lett. B* **362**, 23.
- Kambor, J., C. Wiesendanger, and D. Wyler, 1996, *Nucl. Phys. B* **465**, 215.
- Kampf, K., M. Knecht, J. Novotny, and M. Zdrahal, 2011, *Phys. Rev. D* **84**, 114015.
- Kaptari, L. P., and B. Kampfer, 2008, *Eur. Phys. J. A* **37**, 69.
- Kapusta, J. I., D. Kharzeev, and L. D. McLerran, 1996, *Phys. Rev. D* **53**, 5028.
- Kashevarov, V. L., *et al.* (A2 Collaboration), 2017, *Phys. Rev. Lett.* **118**, 212001.
- Kawarabayashi, K., and N. Ohta, 1980, *Nucl. Phys. B* **175**, 477.
- Kawasaki, M., and K. Nakayama, 2013, *Annu. Rev. Nucl. Part. Sci.* **63**, 69.
- Kelkar, N. G., 2016, *Eur. Phys. J. A* **52**, 309.
- Kelkar, N. G., D. Bedoya Fierro, and P. Moskal, 2016, *Acta Phys. Pol. B* **47**, 299.
- Kelkar, N. G., K. P. Khemchandani, N. J. Upadhyay, and B. K. Jain, 2013, *Rep. Prog. Phys.* **76**, 066301.
- Khoukaz, A., *et al.* (COSY-11 Collaboration), 2004, *Eur. Phys. J. A* **20**, 345.
- Kienle, P., and T. Yamazaki, 2004, *Prog. Part. Nucl. Phys.* **52**, 85.
- Klaja, J., *et al.* (COSY-11 Collaboration), 2010a, *Phys. Rev. C* **81**, 035209.
- Klaja, P., *et al.* (COSY-11 Collaboration), 2010b, *Phys. Lett. B* **684**, 11.
- Klempf, E., and A. Zaitsev, 2007, *Phys. Rep.* **454**, 1.
- Kodaira, J., 1980, *Nucl. Phys. B* **165**, 129.
- Kogut, J. B., and L. Susskind, 1975, *Phys. Rev. D* **11**, 3594.
- Kroll, P., and K. Passek-Kumericki, 2013, *J. Phys. G* **40**, 075005.
- Krusche, B. (CBELSA-TAPS, Crystal Barrel/TAPS Collaborations), 2012, *J. Phys. Conf. Ser.* **349**, 012003.
- Krusche, B., and C. Wilkin, 2015, *Prog. Part. Nucl. Phys.* **80**, 43.
- Kubis, B., and J. Plenter, 2015, *Eur. Phys. J. C* **75**, 283.
- Kupsc, A., 2009, *Int. J. Mod. Phys. E* **18**, 1255.
- Landshoff, P. V., 1994, in *Proceedings of the Summer School on Hadronic Aspects of Collider Physics, Zuoz, Switzerland*, edited by M. P. Locher (Paul Scherrer Institute, Villigen, Switzerland) (PSI-Proceedings 94-01), p. 135.
- Lattimer, J. M., and M. Prakash, 2016, *Phys. Rep.* **621**, 127.
- Lebedowicz, P., O. Nachtmann, and A. Szczurek, 2014, *Ann. Phys. (Amsterdam)* **344**, 301.
- Lepage, G. P., and S. J. Brodsky, 1980, *Phys. Rev. D* **22**, 2157.
- Leutwyler, H., 1998, *Nucl. Phys. B, Proc. Suppl.* **64**, 223.
- Leutwyler, H., 2013, *Mod. Phys. Lett. A* **28**, 1360014.
- Levi Sandri, P., *et al.* (GrAAL Collaboration), 2015, *Eur. Phys. J. A* **51**, 77.
- Liu, Z.-W., W. Kamleh, D. B. Leinweber, F. M. Stokes, A. W. Thomas, and J.-J. Wu, 2016, *Phys. Rev. Lett.* **116**, 082004.
- Mantry, S., M. Pitschmann, and M. J. Ramsey-Musolf, 2014, *Phys. Rev. D* **90**, 054016.
- Mayer, B., *et al.* (SPES2 Collaboration), 1996, *Phys. Rev. C* **53**, 2068.
- Mersmann, T., *et al.* (ANKE Collaboration), 2007, *Phys. Rev. Lett.* **98**, 242301.
- Metag, V., 2015, *Hyperfine Interact.* **234**, 25.
- Metag, V., M. Nanova, and E. Ya. Paryev, 2017, *Prog. Part. Nucl. Phys.* **97**, 199.
- Metag, V., M. Thiel, H. Berghäuser, S. Friedrich, B. Lemmer, U. Mosel, and J. Weil (A2 Collaboration), 2012, *Prog. Part. Nucl. Phys.* **67**, 530.
- Meyer, H. O., *et al.*, 1999, *Phys. Rev. Lett.* **83**, 5439.
- Meyer, H. O., *et al.*, 2001, *Phys. Rev. C* **63**, 064002.
- Michael, C., K. Otnad, and C. Urbach (ETM Collaboration), 2013, *Phys. Rev. Lett.* **111**, 181602.
- Morningstar, C. J., and M. J. Peardon, 1999, *Phys. Rev. D* **60**, 034509.
- Moskal, P., 2004, [arXiv:hep-ph/0408162](https://arxiv.org/abs/hep-ph/0408162).
- Moskal, P., and J. Smyrski (COSY-11 Collaboration), 2010, *Acta Phys. Pol. B* **41**, 2281.
- Moskal, P., M. Wolke, A. Khoukaz, and W. Oelert, 2002, *Prog. Part. Nucl. Phys.* **49**, 1.
- Moskal, P., *et al.* (COSY-11 Collaboration), 1998, *Phys. Rev. Lett.* **80**, 3202.
- Moskal, P., *et al.* (COSY-11 Collaboration), 2000a, *Phys. Lett. B* **474**, 416.
- Moskal, P., *et al.* (COSY-11 Collaboration), 2000b, *Phys. Lett. B* **482**, 356.
- Moskal, P., *et al.* (COSY-11 Collaboration), 2004, *Phys. Rev. C* **69**, 025203.
- Moskal, P., *et al.* (COSY-11 Collaboration), 2006, *J. Phys. G* **32**, 629.
- Moskal, P., *et al.* (COSY-11 Collaboration), 2009, *Phys. Rev. C* **79**, 015208.
- Moskal, P., *et al.* (COSY-11 Collaboration), 2010, *Eur. Phys. J. A* **43**, 131.
- Nagahiro, H., S. Hirenzaki, E. Oset, and A. Ramos, 2012, *Phys. Lett. B* **709**, 87.
- Nagahiro, H., D. Jido, H. Fujioka, K. Itahashi, and S. Hirenzaki, 2013, *Phys. Rev. C* **87**, 045201.
- Nagahiro, H., M. Takizawa, and S. Hirenzaki, 2006, *Phys. Rev. C* **74**, 045203.
- Nakayama, K., J. Haidenbauer, C. Hanhart, and J. Speth, 2003, *Phys. Rev. C* **68**, 045201.
- Nanova, M., *et al.* (CBELSA/TAPS Collaborations), 2012, *Phys. Lett. B* **710**, 600.
- Nanova, M., *et al.* (CBELSA/TAPS Collaborations), 2013, *Phys. Lett. B* **727**, 417.
- Nanova, M., *et al.* (CBELSA/TAPS Collaborations), 2016, *Phys. Rev. C* **94**, 025205.
- Nath, P., and R. L. Arnowitt, 1981, *Phys. Rev. D* **23**, 473.
- Nefkens, B. M. K., *et al.* (Crystal Ball Collaboration), 2005a, *Phys. Rev. C* **72**, 035212.
- Nefkens, B. M. K., *et al.* (Crystal Ball Collaboration), 2005b, *Phys. Rev. Lett.* **94**, 041601.
- Okubo, S., 1962, *Prog. Theor. Phys.* **27**, 949.
- Okubo, S., 1963, *Phys. Lett.* **5**, 165.
- Olbrich, L., M. Ztnyi, F. Giacosa, and D. H. Rischke, 2018, *Phys. Rev. D* **97**, 014007.
- Otnad, K., and C. Urbach (ETM Collaboration), 2018, *Phys. Rev. D* **97**, 054508.
- Papenbrock, M., *et al.* (ANKE Collaboration), 2014, *Phys. Lett. B* **734**, 333.
- Patrignani, C., *et al.* (Particle Data Group) 2016, *Chin. Phys. C* **40**, 100001.
- Peccei, R. D., and H. R. Quinn, 1977, *Phys. Rev. Lett.* **38**, 1440.
- Pena, M. T., H. Garcilazo, and D. O. Riska, 2001, *Nucl. Phys. A* **683**, 322.
- Pendlebury, J. M., *et al.*, 2015, *Phys. Rev. D* **92**, 092003.
- Petren, H., *et al.* (WASA Collaboration), 2010, *Phys. Rev. C* **82**, 055206.
- Pfeiffer, M., *et al.* (TAPS Collaboration), 2004, *Phys. Rev. Lett.* **92**, 252001.
- Pheron, F., *et al.* (Crystal Ball - TAPS Collaborations), 2012, *Phys. Lett. B* **709**, 21.
- Prakhov, S., *et al.* (A2 Collaboration), 2018, *Phys. Rev. C* **97**, 065203.
- Rausmann, T., *et al.* (ANKE Collaboration), 2009, *Phys. Rev. C* **80**, 017001.

- Ringwald, A., 2015, *Proc. Sci. NEUTEL2015*, 021.
- Rodas, A., *et al.* (JPAC Collaboration), 2018, [arXiv:1810.04171](#).
- Roebig-Landau, M., *et al.* (TAPS Collaboration), 1996, *Phys. Lett. B* **373**, 45.
- Rosenberg, L. J., 2015, *Proc. Natl. Acad. Sci. U.S.A.* **112**, 12278.
- Rosenzweig, C., J. Schechter, and C. G. Trahern, 1980, *Phys. Rev. D* **21**, 3388.
- Rosner, J. L., 1983, *Phys. Rev. D* **27**, 1101.
- Rundel, O., M. Skurzok, O. Khreptak, and P. Moskal (WASA-at-COSY Collaboration), 2017, *Acta Phys. Pol. B* **48**, 1807.
- Saghai, B., and Z.-p. Li, 2001, *Eur. Phys. J. A* **11**, 217.
- Saito, K., K. Tsushima, and A. W. Thomas, 2007, *Prog. Part. Nucl. Phys.* **58**, 1.
- Sakai, S., and D. Jido, 2013, *Phys. Rev. C* **88**, 064906.
- Schmidt-Wellenburg, P., 2016, [arXiv:1607.06609](#).
- Schroter, A., E. Berdermann, H. Geissel, A. Gillitzer, J. Homolka, P. Kienle, W. Konig, B. Povh, F. Schumacher, and H. Stroher, 1994, *Z. Phys. A* **350**, 101.
- Senderovich, I., *et al.* (CLAS Collaboration), 2016, *Phys. Lett. B* **755**, 64.
- Shifman, M. A., 1989, *Usp. Fiz. Nauk* **157**, 561 [*Phys. Rep.* **209**, 341 (1991)].
- Shimizu, H. (BGOegg Collaboration), 2017, *Acta Phys. Pol. B* **48**, 1819.
- Shore, G. M., 1998, [arXiv:hep-ph/9812354](#).
- Shore, G. M., 2006, *Nucl. Phys. B* **744**, 34.
- Shore, G. M., 2008, *Lect. Notes Phys.* **737**, 235.
- Shore, G. M., and G. Veneziano, 1992, *Nucl. Phys. B* **381**, 3.
- Shyam, R., 2007, *Phys. Rev. C* **75**, 055201.
- Sigg, D., *et al.*, 1996, *Nucl. Phys. A* **609**, 269; **617**, 526(E) (1997).
- Skurzok, M., P. Moskal, N. G. Kelkar, S. Hirenzaki, H. Nagahiro, and N. Ikeno, 2018, *Phys. Lett. B* **782**, 6.
- Smyrski, J., *et al.* (COSY-11 Collaboration), 2000, *Phys. Lett. B* **474**, 182.
- Smyrski, J., *et al.* (COSY-11 Collaboration), 2007, *Phys. Lett. B* **649**, 258.
- Sun, W., L.-C. Gui, Y. Chen, M. Gong, C. Liu, Y.-B. Liu, Z. Liu, J.-P. Ma, and J.-B. Zhang, 2017, [arXiv:1702.08174](#).
- Suzuki, K., *et al.*, 2004, *Phys. Rev. Lett.* **92**, 072302.
- Szczepaniak, A. P., M. Swat, A. R. Dzierba, and S. Teige, 2003, *Phys. Rev. Lett.* **91**, 092002.
- Tanaka, Y. K., *et al.* (η -PRiME/Super-FRS Collaboration), 2016, *Phys. Rev. Lett.* **117**, 202501.
- Tanaka, Y. K., *et al.* (η -PRiME/Super-FRS Collaboration), 2017, *Acta Phys. Pol. B* **48**, 1813.
- Tanaka, Y. K., *et al.* (η -PRiME/Super-FRS Collaboration), 2018, *Phys. Rev. C* **97**, 015202.
- Thomas, A. W., 1984, *Adv. Nucl. Phys.* **13**, 1.
- Thomas, A. W., and W. Weise, 2001, *The Structure of the Nucleon* (Wiley-VCH, Berlin, Germany).
- Thomas, C. E., 2007, *J. High Energy Phys.* **10**, 026.
- Thompson, D. R., *et al.* (E852 Collaboration), 1997, *Phys. Rev. Lett.* **79**, 1630.
- 't Hooft, G., 1976a, *Phys. Rev. D* **14**, 3432; **18**, 2199(E) (1978).
- 't Hooft, G., 1976b, *Phys. Rev. Lett.* **37**, 8.
- Toki, H., S. Hirenzaki, T. Yamazaki, and R. S. Hayano, 1989, *Nucl. Phys. A* **501**, 653.
- Tomiya, A., G. Cossu, S. Aoki, H. Fukaya, S. Hashimoto, T. Kaneko, and J. Noaki, 2017, *Phys. Rev. D* **96**, 034509; [**96**, 079902 (2017)].
- Tsushima, K., 2000, *Nucl. Phys. A* **670**, 198.
- Tsushima, K., D.-H. Lu, A. W. Thomas, and K. Saito, 1998, *Phys. Lett. B* **443**, 26.
- Urbach, C., 2017, *EPJ Web Conf.* **134**, 04004.
- Vance, S. E., T. Csorgo, and D. Kharzeev, 1998, *Phys. Rev. Lett.* **81**, 2205.
- Veneziano, G., 1979, *Nucl. Phys. B* **159**, 213.
- Vertesi, R., T. Csorgo, and J. Sziklai, 2011, *Phys. Rev. C* **83**, 054903.
- Waas, T., and W. Weise, 1997, *Nucl. Phys. A* **625**, 287.
- Weil, J., U. Mosel, and V. Metag, 2013, *Phys. Lett. B* **723**, 120.
- Weinberg, S., 1978, *Phys. Rev. Lett.* **40**, 223.
- Weinberg, S., 1996, *The quantum theory of fields. Vol. 2: Modern applications* (Cambridge University Press, Cambridge, England).
- Wilczek, F., 1978, *Phys. Rev. Lett.* **40**, 279.
- Wilkin, C., 2014, *Acta Phys. Pol. B* **45**, 603.
- Wilkin, C., 2016, *Acta Phys. Pol. B* **47**, 249.
- Wilkin, C., 2017, *Eur. Phys. J. A* **53**, 114.
- Wilkin, C., *et al.* (ANKE Collaboration), 2007, *Phys. Lett. B* **654**, 92.
- Williams, M., *et al.* (CLAS Collaboration), 2009, *Phys. Rev. C* **80**, 045213.
- Willis, N., *et al.* (SPES3 Collaboration), 1997, *Phys. Lett. B* **406**, 14.
- Witten, E., 1979a, *Nucl. Phys. B* **156**, 269.
- Witten, E., 1979b, *Nucl. Phys. B* **149**, 285.
- Witten, E., 1980, *Ann. Phys. (N.Y.)* **128**, 363.
- Witthauer, L., *et al.* (A2 Collaboration), 2016, *Phys. Rev. Lett.* **117**, 132502.
- Witthauer, L., *et al.* (A2 Collaboration), 2017, *Phys. Rev. C* **95**, 055201.
- Wronska, A., *et al.* (ANKE Collaboration), 2005, *Eur. Phys. J. A* **26**, 421.
- Wycech, S., and W. Krzemiński, 2014, *Acta Phys. Pol. B* **45**, 745.
- Xie, J.-J., W.-H. Liang, E. Oset, P. Moskal, M. Skurzok, and C. Wilkin, 2017, *Phys. Rev. C* **95**, 015202.
- Yamazaki, T., *et al.*, 1996, *Z. Phys. A* **355**, 219.
- Yorita, T., *et al.*, 2000, *Phys. Lett. B* **476**, 226.
- Zweig, G., 1964, CERN Report No. TH-412.